



Age, depositional history and tectonics of the Indo-Myanmar Ranges, Myanmar

Tin Tin Naing¹, Stuart A. Robinson^{1*}, Mike P. Searle¹, Chris K. Morley², Ian Millar³, Owen R. Green¹, Paul R. Bown⁴, Taniel Danelian⁵, Maria Rose Petrizzo⁶ and Gideon M. Henderson¹

¹ Department of Earth Sciences, University of Oxford, South Parks Road, Oxford OX1 3AN, UK

² Department of Geological Sciences, Chiang Mai University, 239 Huaykaew Road, Chiang Mai 50200, Thailand

³ BGS Keyworth, Nottingham NG12 5GG, UK

⁴ Department of Earth Sciences, University College London, Gower Street, London WC1E 6BT, UK

⁵ Université Lille, CNRS, UMR 8198 – Evo-Eco-Paleo, F-59000 Lille, France

⁶ Dipartimento di Scienze della Terra ‘A. Desio’, Università degli Studi di Milano, via Mangiagalli 34, 20133 Milano, Italy

SAR, 0000-0003-4329-1058

* Correspondence: stuart.robinson@earth.ox.ac.uk

Abstract: The Indo-Myanmar Ranges make up an enigmatic mountain belt occupying a complex tectonic zone in western Myanmar, extending from the northern continuation of the active Sunda–Andaman arc into the eastern Himalayan Syntaxis. The Indo-Myanmar Ranges are part of an accretionary forearc basin–arc complex that includes the Central Myanmar Basin and the Wuntho–Popa Arc to the east. New biostratigraphic, petrological and detrital zircon U–Pb age data are presented and used to test and refine the divergent tectonic models that have been proposed for western Myanmar. These data suggest that: (1) the Upper Triassic Pane Chaung Formation was originally deposited adjacent to the NE Indian continental margin within northern Gondwana during the Late Triassic; and (2) the Upper Cretaceous–Paleogene rocks of the Indo-Myanmar Ranges were mainly derived from the Wuntho–Popa Arc and Inner Belt, with a subordinate input from a crustal source, potentially from the Naga metamorphic-type Paleozoic basement. The Kalemio Ophiolite has an Early Cretaceous age similar to the ages of ophiolites in the Indus–Yarlung Tsangpo Suture Zone, south Tibet and Nagaland, reinforcing the hypothesis that they were once part of the same Neotethyan ocean floor.

Supplementary material: Sample locality details, detailed methodologies and geochemical data are available at <https://doi.org/10.6084/m9.figshare.c.6487105>

Received 24 June 2022; revised 10 March 2023; accepted 26 March 2023

The Indo-Myanmar Ranges (IMR), also known as the ‘Indo-Burma Ranges’, form an enigmatic mountain belt running the length of western Myanmar, extending into India and Bangladesh. To the SW lies the Indian Ocean and to the east lies the Central Myanmar Basin (CMB) and the Wuntho–Popa Arc (WPA) (Fig. 1). The IMR connect the Himalayan orogen to the north with the Sumatra–Andaman Trench to the south (Fig. 1). Rangin *et al.* (2013) proposed the existence of a so-called Burma (Myanmar) microplate, which includes the IMR, the complex core of the IMR and the CMB. A major belt of ophiolites and deep-marine sediments, including the Nagaland and Kalemio ophiolites, separates the IMR to the west from the CMB to the east, splitting the microplate. The tectonics of the Myanmar microplate are dominated by the oblique, north- to NE-directed subduction of Tethyan oceanic crust beneath Asia and the subsequent clockwise rotation caused by the indenting Indian plate to the west. The Myanmar microplate obliquely accreted with NE India as it moved northwards and underwent considerable strike-slip translation (Rangin *et al.* 2013; Rangin 2017, 2018). However, the details of how deformation evolved within the IMR, how much dextral strike-slip translation has affected the region, and the tectonic context and timing of the emplacement of the fragments of oceanic crust all remain controversial. The IMR has been interpreted in the context of originally north- to NE-directed subduction during the Mesozoic–Cenozoic (Mitchell 1993; Westerweel *et al.* 2019). Like the Indus–Yarlung Tsangpo Suture Zone (IYTSZ) (e.g. Hébert *et al.* 2012; Kapp and DeCelles 2019), the IMR contains an important record of

the Neotethys subduction history that can be used to test and refine Mesozoic–Cenozoic plate reconstructions.

The origin and tectonic affinity of the IMR remain open to multiple interpretations. Some earlier workers considered that the west-verging IMR sediments were an accretionary prism formed during the subduction of various stages of the Tethys Ocean beneath the Eurasian plate and postulated that sediment was sourced from the emerging Himalaya to the north (Curry *et al.* 1979; Bender 1983; Hutchinson 1989; Curry 2005). More recent studies of the IMR dispute this view and infer a much more complex tectonic setting (see review in Morley *et al.* 2020). Some workers have interpreted the IMR as the main India–Asia suture zone, marked by a discontinuous belt of ophiolites, including the Naga Hills Ophiolite in the northern IMR in NE India (Acharyya 2007; Singh 2013; Ghose *et al.* 2014) and the Kalemio Ophiolite in the Chin Hills of the eastern IMR (Liu *et al.* 2016b).

Several palaeogeographical reconstructions have been proposed for western Myanmar that can be summarized in two groups. According to the first group of models, the West Myanmar Terrane (WMT), including the CMB and the WPA (also known as the West Burma Terrane) was part of SE Asia by the Early Mesozoic and the IMR developed on this margin. These models support suggestions that the IMR were part of Gondwanan Sibumasu Terrane or the Cathaysian West Sumatra Terrane (e.g. Mitchell 1992; Barber and Crow 2005, 2009; Hall 2009; Metcalfe 2011; Hall 2012; Morley 2012, 2018; Metcalfe 2013; Hall 2014). In the second group of models, a West Myanmar microplate (Mt Victoria Land) separated

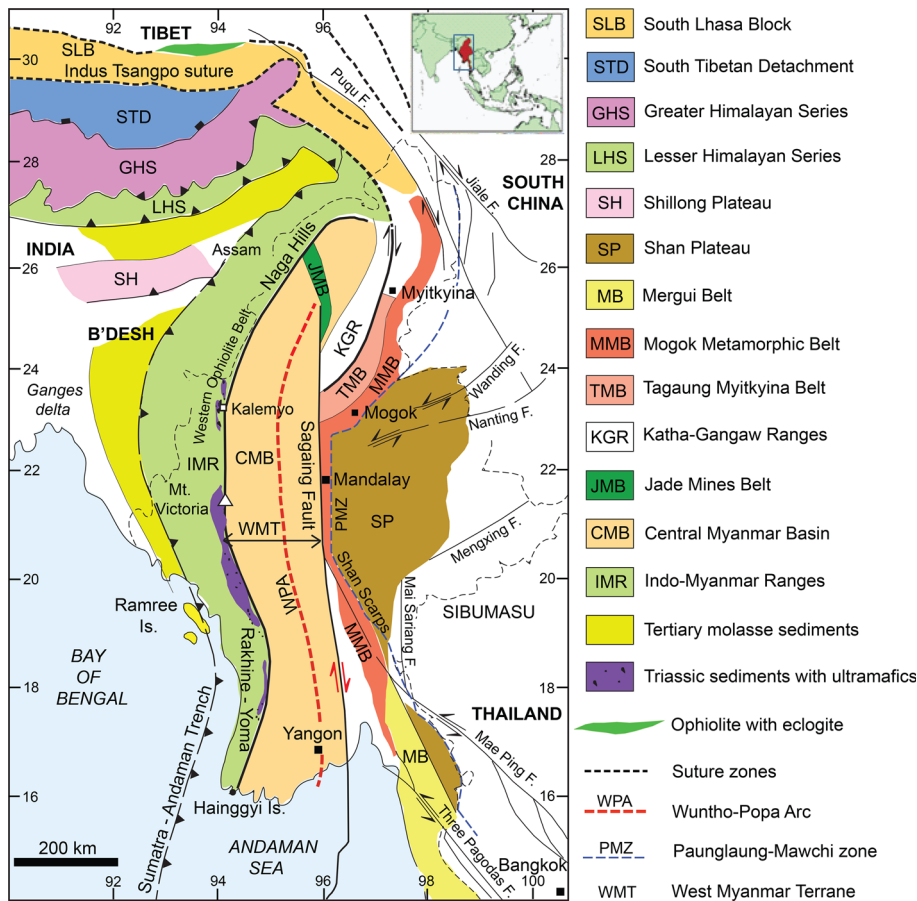


Fig. 1. Simplified geological map of Myanmar (Burma) from the eastern Himalayan Syntaxis south to Mergui. Source: modified after Searle *et al.* (2007).

from Western Australia in the Jurassic and was added to the WMT, and therefore SE Asia, in the Cretaceous (e.g. Mitchell 1986, 1989; Sengör 1987; Veevers 1988; Metcalfe 1990; Audley-Charles 1991). More recently, the palaeo-position of West Myanmar has been tested using provenance data (particularly detrital zircon U–Pb ages and geochemistry) applied to Triassic deep-water sediments (the Pane Chaung Formation) in the IMR. Sevastjanova *et al.* (2016) suggested that West Myanmar was part of SE Asia before the Triassic–Early Cretaceous Indosinian Orogeny and that it is of neither Cathaysian nor Indian plate affinity. Another model argues that the detrital zircon ages of the Pane Chaung Formation are comparable with NW Australia and Greater India and that they were all deposited during the Late Triassic on a submarine fan that developed along the north and NW margins of Australia (Cai *et al.* 2016; Yao *et al.* 2017).

An additional constraint on tectonic reconstructions is a recent palaeomagnetic study of Upper Cretaceous igneous and Eocene sedimentary rocks from the northern part of the terrane, which indicates a position at *c.* 5° S in the Late Cretaceous and at *c.* 4° N in the Late Eocene (Westerweel *et al.* 2019). Palaeomagnetic data from additional Cenozoic sites in the CMB that constrain the location of strata of different ages are consistent with these 2019 data (Westerweel 2020). A key problem with the WMT is that much of it is covered by Cenozoic deposits and therefore the outcrops of Mesozoic and Paleozoic units are geographically restricted. It possibly developed through multiple collisions of tectonic blocks and is a composite terrane (see Morley *et al.* 2021 for a discussion). For example, palaeomagnetic data constraints can be accommodated in the Late Triassic submarine fan model for northern Gondwana (Cai *et al.* 2016; Yao *et al.* 2017) if a continental fragment (Mt Victoria Land; Mitchell 1993) collided with a volcanic arc (the WMT) during the Early Cretaceous (see discussion in Licht *et al.* 2020; Morley *et al.* 2020, 2021).

Fundamental challenges to understanding the IMR include: historically highly limited access along rudimentary roads and trails; limited exposures in high-relief terrain covered by forest and restriction of outcrops to river courses; the highly complex structure; and the extensive, highly monotonous marine facies known as flysch units with a broad age range (Triassic–Paleogene) and limited biostratigraphic age control (e.g. Brunnenschweiler 1966; Bannert *et al.* 2011). At the time of our fieldwork (2016), access to some parts of the Rakhine coastal area was prohibited or restricted. Road-building has created some new outcrops and some excellent exposures exist along river sections. U–Pb dating of zircons and other dating methods have been applied to understand the timing of the tectonic, igneous and metamorphic events and the stratigraphy (see review in Sevastjanova *et al.* 2016; Liu *et al.* 2016a; Yao *et al.* 2017; J.E. Zhang *et al.* 2017; J. Zhang *et al.* 2018; Bandopadhyay *et al.* 2022; Najman *et al.* 2022).

Understanding the tectonic evolution of the IMR requires a knowledge of its prior location, when and where it separated from Gondwana, and when and how it collided with SE Asia. Disagreement still remains regarding the presence and extent of continental basement in the IMR (see discussions in Morley *et al.* 2020, 2021). Furthermore, many existing lithological correlations are solely based on comparable lithologies and remain untested using geochronological techniques. We present here the results of biostratigraphic, petrographic, detrital zircon U–Pb age and Hf isotope investigations of the Triassic–Paleogene flysch sandstones in the IMR of western Myanmar. The existing U–Pb age data along the IMR are also reviewed. Our aim is to constrain the stratigraphic ages, interpret the palaeoenvironmental significance, structural and tectonic history of the rocks from the IMR, and to aid the palaeogeographical reconstruction of western Myanmar. Three major points of interest are discussed: (1) the palaeogeographical location of the Pane Chaung Formation during its deposition; (2) the

ages of the ophiolites and the associated radiolarian cherts and mélange; and (3) the timing of suturing between India and the WMT (the closure of the Neotethys Ocean).

Geological background

Regional geology of Myanmar

Myanmar is located on the eastern edge of the indenting India plate and forms a southeastwards continuation of the Himalayan orogenic belt, south of the eastern Himalayan Syntaxis. Myanmar is a transition between the continental collision along the Himalaya in the north and the active Indian Ocean subduction beneath the Sunda Arc (the Sumatra–Andaman Trench) in the south (e.g. Mitchell 1993; Curray 2005; Morley 2009; Morley and Searle 2017). Geologically, Myanmar can be subdivided into three north–south-trending tectonic belts (Fig. 1). The Shan Plateau is part of the Sibumasu Terrane, whereas the CMB is associated with the so-called WMT, west of the Sagaing Fault. The IMR are juxtaposed along the western margin of the CMB. This investigation concentrated on the two western belts.

The CMB lies between the Sagaing Fault and the IMR and extends southwards to the Andaman Sea. It is composed of a thick succession of Upper Cretaceous–Pleistocene marine and fluvial sediments locally overlain by Pliocene–Quaternary calc-alkaline volcanics (e.g. Pivnik *et al.* 1998; Mitchell *et al.* 2010; Licht *et al.* 2016). The CMB has traditionally been subdivided into Late Cretaceous–Cenozoic western forearc and eastern back-arc basins (Pivnik *et al.* 1998), separated by the WPA (Mitchell *et al.* 2012; Gardiner *et al.* 2015). The basin is bounded by two major faults: the long, linear, dextral strike-slip Sagaing Fault, the trace of which is clearly expressed in satellite images, located along the eastern margin of the CMB (e.g. Tun and Watkinson 2017); and the dextral Kabaw Fault along the western margin, the trace of which is possibly discontinuous and less clearly expressed in satellite images (e.g. Morley *et al.* 2020).

The IMR lie west of the CMB and are composed of a thick imbricated thrust succession of Mesozoic and Cenozoic flysch deposits associated with several large and numerous smaller ophiolite fragments. The ophiolites in the IMR (in particular the Kalemio area) and India (Nagaland) are interpreted as Penrose-type obducted ophiolites (e.g. United Nations 1979; Mitchell 1993; Socquet *et al.* 2002; Acharyya 2007; Rangin 2018) or accretionary-type ophiolites (e.g. Harlow *et al.* 2015; Fareeduddin and Dilek 2015; Barber *et al.* 2017; Hla *et al.* 2017). The ophiolites consist of small, highly dismembered bodies of ultramafic rocks up to c. 10 km long (north–south), together with smaller bodies of pillow lavas and gabbros (Mitchell 1993; Mitchell *et al.* 2010; J.E. Zhang *et al.* 2017; J. Zhang *et al.* 2018; Morley *et al.* 2020). The largest serpentinized peridotite body (Webula; Fig. 2d) has a low-angle thrust at its base (Brunnschweiler 1966) and a small patch of metamorphic sole rocks outcrops at its southern end (J.E. Zhang *et al.* 2017). The basal thrusts of three of the peridotite bodies in the Kalemio area are estimated to dip east between 10° and 34° and underwent top-to-the-west displacement (Morley *et al.* 2020). Sheared mélanges, with matrices of mudrock or serpentinite, are sometimes juxtaposed with the ultramafic rocks (United Nations 1979; Mitchell *et al.* 2010; J. Zhang *et al.* 2018; Morley *et al.* 2020) and these dismembered and thrust ophiolite-association rocks are present within the belt of Kanpetlet Schists and the Pane Chaung Formation. The earlier thrusting and folding is overprinted by swarms of closely spaced, later (Cenozoic?), c. north–south-trending dextral strike-slip faults (Morley *et al.* 2020). The ophiolite fragments define a north–south suture zone that separates the IMR to the west from the CMB to the east. The IMR form an active fold–thrust belt above an east-dipping active subduction zone, along

which numerous earthquakes occur (e.g. Steckler *et al.* 2016; Searle *et al.* 2017; Sloan *et al.* 2017). As the main focus of this paper, the IMR are described in more detail in the following sections.

Indo-Myanmar Ranges

The IMR constitute a north–south-trending, c. 1300 km long arcuate fold–thrust belt (Fig. 1). They lie on the eastern margin of the highly oblique convergent zone that extends from the collisional Himalayan region in the north to the subduction-related Sumatra–Andaman Trench in the south (Acharyya 2015). Published accounts indicate that the IMR initially formed in an accretionary prism setting during the Jurassic–Early Eocene, then began to evolve during the Late Eocene into a subaerial fold–thrust belt after the collision between Sundaland and the Indian plate (e.g. Theobald 1871; Chhibber 1927, 1934; Brunnschweiler 1966, 1974; Mitchell 1993; Maurin and Rangin 2009; Mitchell *et al.* 2010; Bannert *et al.* 2011; Rangin *et al.* 2013; Rangin 2017).

The IMR belt consists of a thick sequence of westward-younging Mesozoic–Cenozoic flysch deposits associated with several large, and numerous small, ophiolite fragments. Low-grade greenschist facies metamorphic rocks to the east reflect a minor amount of crustal thickening (Brunnschweiler 1966; Socquet *et al.* 2002; Bannert *et al.* 2011; Morley *et al.* 2020). The thick Mesozoic–Cenozoic flysch deposits of the IMR are typically poorly fossiliferous and are difficult to differentiate due to their monotonous nature, particularly in the Inner Belt (Brunnschweiler 1966; Bannert *et al.* 2011). The reworking of older fossils into younger deposits is common (Brunnschweiler 1966; United Nations 1979), making biostratigraphic resolution complicated.

The ranges are flanked to the east by the CMB and to the west by basins in eastern Bangladesh and NE India (e.g. Ghose *et al.* 2014; Steckler *et al.* 2016). The eastward extent of the oldest part of the IMR is obscured by the Upper Cretaceous–Recent sedimentary cover of the CMB (forearc basin). Traditionally, the IMR have been divided into Inner and Outer belts (e.g. United Nations 1979; Mitchell *et al.* 2010). Maurin and Rangin (2009) refer to the Eastern Belt as the core of the IMR and subdivide the Western Belt into an Inner Belt and a westernmost Outer Belt. The Central and the Inner belts are separated by the Lelon Fault (Maurin and Rangin 2009) and by the transpressional Kheng Fault (Mitchell *et al.* 2010; Mitchell 2017). The Inner and Outer belts are divided by the strike-slip Kaladan Fault (Maurin and Rangin 2009). The Outer Belt is composed of Neogene sediments, whereas the Inner Belt consists of predominantly Upper Cretaceous–Paleogene sediments. The central part of the IMR is a tectonically complex zone, marking a broad suture zone containing units derived from the Tethys Ocean and related back-arc basins consisting of materials related to the oceanic crust (including large and small bodies of ultramafic rocks and serpentinite, pillow lavas, radiolarian chert and mélange), Upper Triassic flysch (the Pane Chaung Formation) and metamorphic units, including fragments of a metamorphic sole to the ultramafic bodies. A larger region of low-grade to greenschist facies metamorphic rocks, the Kanpetlet Schists (Fig. 2b), crops out in the Southern Chin Hills area (United Nations 1979; Socquet *et al.* 2002).

Ophiolites

The ophiolitic rocks are best preserved along the eastern margin of the IMR, from the Naga Hills in the north to the Andaman Islands in the south, and are referred to as the Western Ophiolite Belt (Mitchell *et al.* 2010; Acharyya 2015; Hla *et al.* 2017; Morley and Searle 2017). These ophiolites are generally interpreted to represent the eastern suture of the Indian plate (Mitchell 1981; Acharyya 1986; Searle *et al.* 2017). The ophiolite belt contains blocks of peridotite,

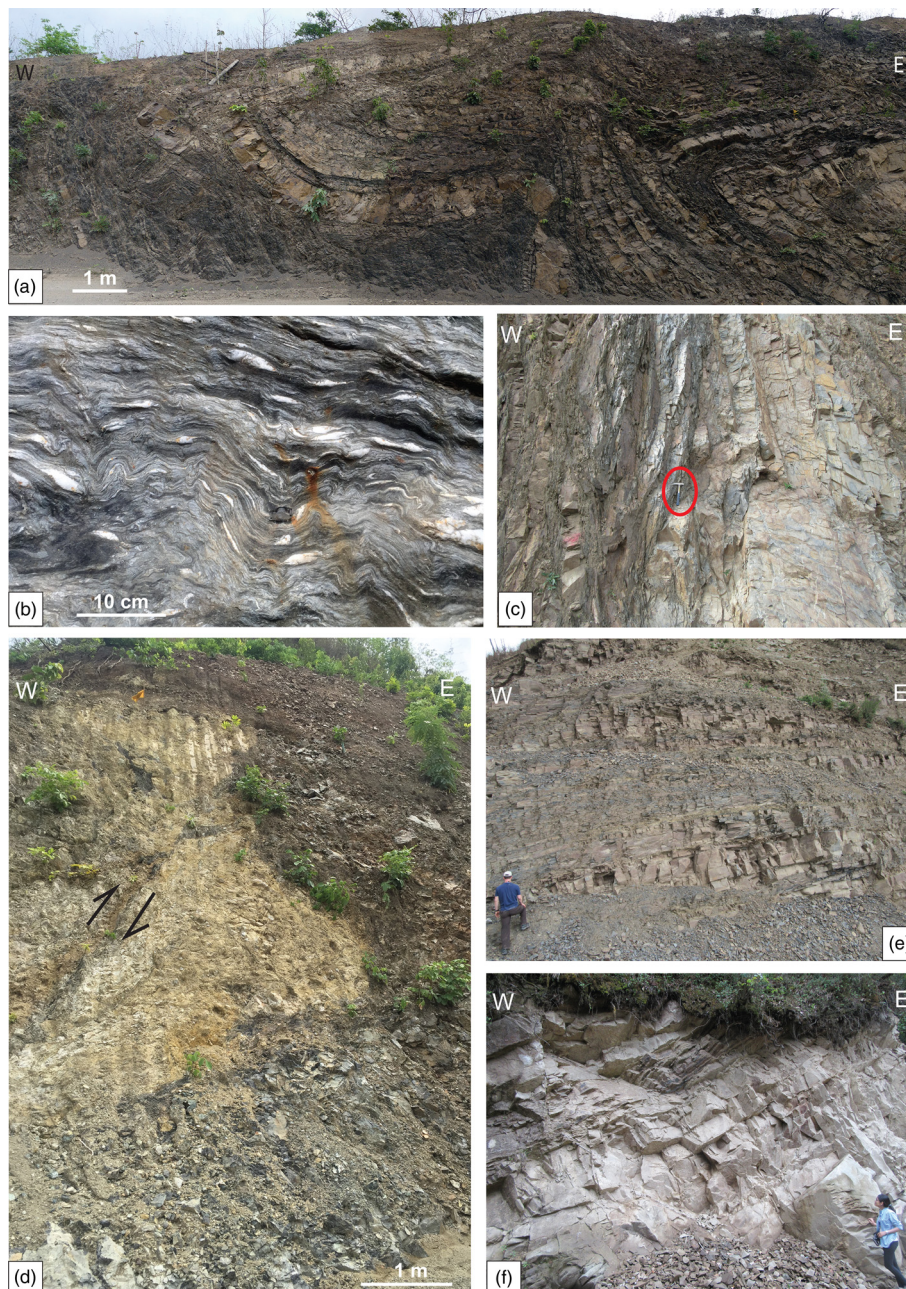


Fig. 2. Field photographs of outcrops sampled in the Indo-Myanmar Ranges. (a) Refolded recumbent fold in the Pane Chaung Formation, Mindat Road. (b) Kanpetlet Schists, Saw River. (c) Subvertical bedding in the Falam Formation, Kalemmyo–Falam Road. Red circle shows location of hammer. (d) Webula, serpentinitized harzburgite offset by a strike-slip fault of probable Cenozoic age. (e) Paleocene–Eocene Chunsang Formation, Falam–Kennedy Road. (f) Eocene Kennedy Sandstone, Kennedy Peak.

gabbro, pillow basalt, radiolarian chert and some metamorphic rocks within a matrix of serpentinite (Mitchell 1993; Acharyya 2007, 2015; Bannert *et al.* 2011; Ghose *et al.* 2014; Liu *et al.* 2016b; Hla *et al.* 2017; J.E. Zhang *et al.* 2017). Three major peridotite massifs occur in the Chin Hills: Mwe Taung, Bophi Vum and Webula. The mantle peridotites mainly consist of harzburgites, with minor lherzolites and dunites. There are some associated massive chromite-bearing bodies, particularly around Mwe Taung. The gabbros are limited in extent and several exposures (small-sized blocks <10 m²) in the Mindat and Yazagyo area occur in a serpentinite matrix (J.E. Zhang *et al.* 2017; J. Zhang *et al.* 2018; Morley *et al.* 2020). The best exposed ophiolitic mélange is found in the spillway area of the Yazagyo Dam, where an ultramafic klippe overlies Triassic flysch (J. Zhang *et al.* 2018). The spillway outcrops reveal a mélange, the blocks of which include bedded red cherts, limestones and serpentinite, sheared together with basalts that probably represent the down-going plate (J. Zhang *et al.* 2018; Morley *et al.* 2020). In Khwekha, a low-grade metamorphic mélange unit, overlain by a greenschist- to amphibolite-grade

metamorphic sole, occurs below the southern outcrops of the Webula Ophiolite (Hla *et al.* 2017).

The U–Pb dates of magmatic zircons in gabbros and rodingites from the ophiolitic mélange in Kalemmyo yield Early Cretaceous ages, ranging between 126 ± 2 and 133 ± 2 Ma (Liu *et al.* 2016b; J. Zhang *et al.* 2018). These Early Cretaceous ages are inferred to represent the age of oceanic crust formation (Searle *et al.* 2017), with the ophiolite forming above an intra-oceanic subduction zone (Liu *et al.* 2016b). For the Nagaland Ophiolite, Singh *et al.* (2017) obtained zircon U–Pb ages from plagiogranites of 116 ± 2 to 118 ± 1 Ma and similar ages have been reported for ophiolitic gabbros in Manipur (Aitchison *et al.* 2019). Late Jurassic (Kimmerigian–Late Tithonian) radiolarians occur in a chert block in the mélange in Nagaland (Baxter *et al.* 2011), with both Jurassic and Early Cretaceous radiolarians occurring in red and green cherts, respectively, in Manipur. Notably, the cherts occur in association with basalts of mid-ocean ridge basalt affinity and are considered to present fragments scrapped off from the lithospheric slab subducting beneath the ophiolite.

U–Pb zircon ages of 115 ± 1 to 119 ± 3 Ma from amphibolites at Kalemmyo are interpreted as part of a metamorphic sole to the ophiolite and thus indicate the timing of its emplacement within an accretionary prism (Liu *et al.* 2016b; J.E. Zhang *et al.* 2017; Morley *et al.* 2020). Some workers have suggested that ophiolite fragments were emplaced prior to the deposition of Aptian–Cenomanian limestones (United Nations 1979; Mitchell 1993; Mitchell *et al.* 2010). Geochemical studies indicate that the mafic volcanic rocks included within the mélange have a range of mid-ocean ridge and supra-subduction zone affinities (within an accretionary prism (Liu *et al.* 2016b; Singh *et al.* 2017; Niu *et al.* 2018). Searle *et al.* (2017) considered the IMR to contain at least two different ophiolites: (1) a more westerly zone that involves ophiolite fragments embedded into the Cenozoic section and emplaced during the Paleogene in the Naga–Manipur region (Ghose *et al.* 2014; Aitchison *et al.* 2019); and (2) a more easterly zone of ophiolites emplaced prior to the mid-Cretaceous, closely associated with overthrust Triassic sediments (the Pane Chaung Formation) and metamorphic rocks (the Kanpetlet Schists, Nimi Formation), which are unconformably overlain by the Upper Cretaceous Paung Chaung and Kabaw formations. In the northern half of the IMR the Naga Ophiolites are overthrust by various Paleozoic units attributed to the Naga Metamorphic Complex (Brunnschweiler 1966; Aitchison *et al.* 2019), where the metamorphic rocks occur above and below folded and thrust fragments of ophiolites on both the western and eastern margins of the Chindwin Basin, including the Jade Belt region (Brunnschweiler 1966; Htay *et al.* 2017).

Sedimentary and meta-sedimentary units of the IMR

The primary stratigraphic units in the core of the IMR are thick sequences of turbidites (flysch) assigned to the Triassic Pane Chaung Formation, the Kanpetlet Schists and related metabasites, together with fragments of ophiolites, including gabbros, ultramafic rocks, radiolarian cherts and pillow lavas (e.g. United Nations 1979; Mitchell 1993, 2017). Despite strong thrusting, strike-slip deformation and folding, the Pane Chaung Formation is seen to grade into greenschist-grade Kanpetlet Schists along some river sections (United Nations 1979; Maurin and Rangin 2009; Bannert *et al.* 2011). The age of the Kanpetlet Schists was originally considered to be pre-Mesozoic (Brunnschweiler 1966) or Triassic (Socquet *et al.* 2002). More recently obtained detrital zircon age data indicate a Triassic or younger age (J.E. Zhang *et al.* 2017; Najman *et al.* 2020).

The Pane Chaung Formation is widely exposed along the eastern flank of the Chin Hills outwards to the Rakhine area and is composed of indurated turbiditic sandstones and shales (Fig. 2a). The Triassic depositional age of the Pane Chaung Formation is based on the rare occurrence of *Halobia* fossils (Gramann 1974; United Nations 1979; Bannert *et al.* 2011; Yao *et al.* 2017; J.E. Zhang *et al.* 2017). However, identification of the Pane Chaung Formation is commonly based on lithological characteristics across large tracts of the IMR, without any supporting fossil evidence. The discontinuous nature of outcrops in the IMR, and the lithologically similar overlying Cretaceous units, generates considerable uncertainty when mapping the Pane Chaung Formation (Brunnschweiler 1966; Bannert *et al.* 2011). The limited fossil occurrences prevent the resolution of the full age range of the formation. Recent detrital zircon analysis (Sevastjanova *et al.* 2016; Yao *et al.* 2017) indicates that the maximum depositional ages are predominantly Late Triassic, with some Early Jurassic ages, and help to address the difficulties in correlation.

IMR Inner Belt

The thick Mesozoic–Cenozoic flysch deposits of the IMR are typically poorly fossiliferous and difficult to differentiate

(Brunnschweiler 1966; Bannert *et al.* 2011). In the central area of the IMR, along the Kalemmyo–Falam and Webula–Falam road sections, the Triassic Pane Chaung Formation is apparently unconformably overlain by the Upper Cretaceous Falam Formation (Mitchell *et al.* 2010) (Fig. 2c). The latter is remarkably monotonous, composed of mudstones with minor fine-grained turbidite sandstones and exotic *Globotruncana* limestone blocks (Brunnschweiler 1966; United Nations 1979). The Falam Formation is stratigraphically overlain by the Chunsang Formation (United Nations 1979). Biostratigraphic data for the Chunsang Formation indicate that it is Paleocene to Lower Eocene and is probably equivalent to part of the Disang Group of Assam (Mitchell *et al.* 2010; Mitchell 2017). Lokho *et al.* (2020) recorded Planktonic Foraminiferal Zones E14–16 correlative to the upper middle to upper Eocene in the Upper Disang Formation. The Chunsang Formation passes stratigraphically up into the Kennedy Sandstone (Fig. 2e, f) of probable Eocene age (Mitchell *et al.* 2010; Mitchell 2017). In the more southerly Rakhine area of the IMR, the geological team of the United Nations (1979) mapped the Padaung–Taungup road section as Upper Cretaceous–Paleogene flysch, which may be laterally equivalent to (part of?) the Falam Formation, Chunsang Formation and Kennedy Sandstone further north. However, this area in Rakhine consists almost entirely of a thick, monotonous succession of sandstone and mudstone flysch units with no obvious stratigraphic division, either in the field or on aerial photographs. Limestones with *Globotruncana* are common as exotic blocks.

IMR Outer Belt

The Outer Belt crops out in the furthest western parts of the IMR, as well as on the offshore islands of the Rakhine coast, and continues along strike into Bangladesh (Fig. 1). It is predominantly composed of Neogene flysch-type sediments with minor deformed Campanian–Maastrichtian pelagic limestones and mudstones, assumed to be olistoliths (Bender 1983; Mitchell 1993; Allen *et al.* 2008). Sediments in the Outer Belt range from the Miocene and, furthest west, are Miocene to Pleistocene (Maurin and Rangin 2009; Khin *et al.* 2017). Maurin and Rangin (2009) noted that the Outer Belt is affected by the detached fold–thrust system.

Materials and methods

Three sampling campaigns were undertaken in the Rakhine, Mt Victoria and Kalemmyo areas of the IMR in 2016, 2017 and 2018 (Figs 3a, b, 4a and 5a). Fieldwork was conducted to sample many of the Triassic–Eocene exposures in the IMR for biostratigraphic, petrographic and geochemical analyses. Biostratigraphy was used to ascertain the depositional ages of the sediments. The petrographic and geochemical data presented here provide insights into the origins of the sediments and better inform palaeogeographical reconstructions. Structural orientation and fault kinematic data were collected in the field (Figs 3b, 4a and 5a) and local and regional cross-sections were constructed (Figs 4b, 5b). The field relationships between different units were investigated (Fig. 2). These data are also provided in Morley *et al.* (2020).

Samples

In the Rakhine area, samples were collected along the Padaung–Taungup and Gwa road sections and the Rakhine coastal area (Fig. 3b). In the Mt Victoria area, sample collection was carried out along the Saw to Mt Victoria road, the main Mindat–Kyaukhtu road, the Mindat–Kanpetlet road and the Saw River (Fig. 4a). In the Kalemmyo area, samples were collected along the Kalemmyo–Falam–Kennedy Peak road, the Wabula Taung–Falam road and the

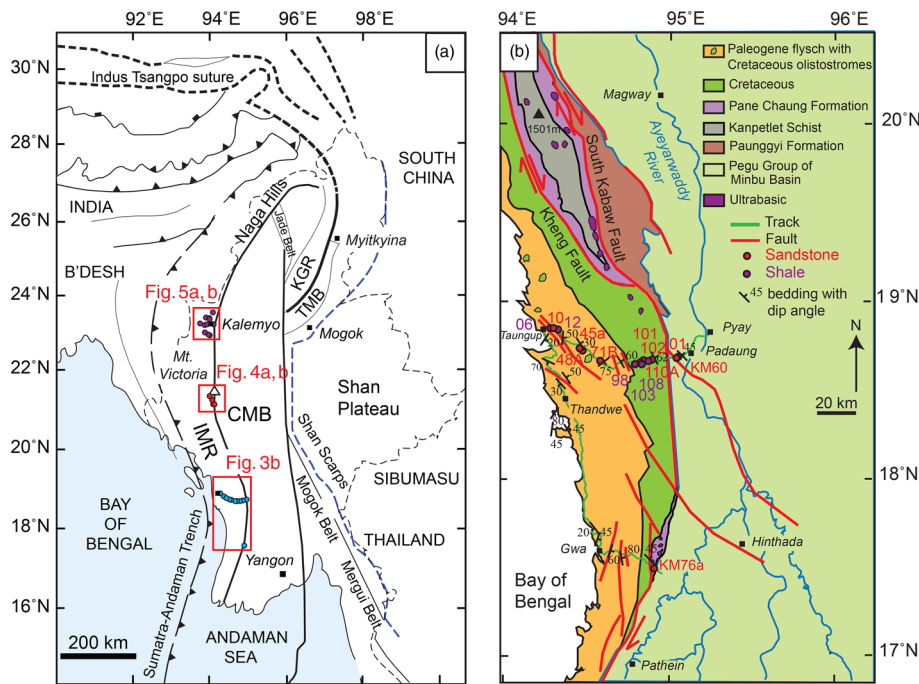


Fig. 3. (a) Simplified geological map of Myanmar (Burma). Black dots show sample locations and squares show location of study areas. (b) Outline geological map of the Rakhine area showing the broadscale distribution of the geological units and sample locations. For simplicity, the prefix ‘IBR’ is omitted from all sample labels on the map. Source: part (b) modified from [United Nations \(1979\)](#). KGR, Katha–Gangaw Range; TMB, Tagaung–Myitkyina Belt; CMB, Central Myanmar Basin; IMR: Indo-Myanmar Range.

Kalemyo–Kalewa road (Fig. 5a). Sample location details are presented in [Supplementary data file 1](#).

Techniques

The analytical methods are summarized in the following sections and provided in full, together with all data tables, in the [Supplementary Material](#).

Biostratigraphy

Shale samples were prepared for foram analysis using a freeze–thaw technique. Four chert samples (KM37, KM37b, KM39a and KM39b) were collected from the ophiolitic mélangé at the Yazagyo Dam in the core of the IMR. They were prepared at the University of Oxford using standard radiolarian extraction techniques for cherts with the use of dilute hydrofluoric acid ([Pessagno and Newport 1972](#); [De Wever *et al.* 2001](#)). The planktonic foram taxonomy followed the pforams@mikrotax database at <http://www.mikrotax.org/pforams> ([Huber *et al.* 2016](#)) and [Huber *et al.* \(2022\)](#).

Petrography

Thin section petrographic analyses were performed on 20 sandstones following the Garzanti classification ([Garzanti 2016](#)) and Gazzi–Dickinson methods ([Dickinson 1985](#)). A minimum of 500 grains (including matrix and cement) were counted per thin section and mineralogical compositions were recalculated on a matrix-free basis prior to plotting the essential components.

Detrital zircon U–Pb and Hf isotope analysis

The U–Pb age determinations were undertaken at the Geochronology and Tracers Facility of the British Geological Survey (Keyworth, UK). U–Pb analyses were carried out on 24 samples using a multi-collector Nu Plasma HR mass spectrometer coupled to a New Wave 193SS solid-state laser. Six sandstone samples from the Upper Cretaceous–Eocene flysch unit were then selected for Hf isotope analysis using a Thermo Scientific Neptune mass spectrometer coupled to a New Wave Research UP193UC Excimer laser ablation system. Details of reference materials and analytical methods are given in [Supplementary File 2](#).

Results

Biostratigraphy

The Cretaceous–Paleogene flysch units of the Inner Belt are highly monotonous and it is difficult to differentiate between the Cretaceous and Eocene strata. We attempted to establish new, more robust, biostratigraphic control for this region based on forams and nannofossils extracted from 11 shale samples. However, only samples IBR06, IBR12, IBR98, IBR103 and IBR108 yielded rare forams and nannofossils. Three samples mapped as Cretaceous (IBR98, IBR103 and IBR108; Fig. 3b) contain *Planoheterohelix globulosa* (Ehrenberg), *Planohedbergella ultramicro* (Subbotina) and *Muricohedbergella planispira* (Tappan) (Fig. 6a–d). Nannofossils adhered to planktonic forams in sample IBR98 were identified by co-author Paul Bown in scanning electron microscopy images as *Prediscosphaera columnata* (Stover) and *Watznaueria* sp. (Fig. 6g, h). The planktonic forams indicate an Albian–Maastrichtian range, whereas the nannofossils indicate correlation with the Albian–Turonian. Two samples mapped as Paleogene (IBR06 and IBR12; Fig. 3b), including *Chiloguembelina wilcoxensis* (Cushman & Ponton) and *Chiloguembelina ototara* (Finlay) (Fig. 6e, f), did not yield any nannofossils. The planktonic foram assemblage is assigned to the Paleocene–Eocene. Despite these rare identifications, there are simply too few occurrences of fossils from the shales in the Inner Belt to be sure of the full stratigraphic range of these sediments.

In the Yazagyo Dam section, abundant and well-preserved radiolarians were obtained from sample KM37b with the most significant taxa being illustrated in Fig. 7. The occurrence of *Zhamoidellum ovum* (Dumitrica) and *Fultacapsa sphaerica* (Ozoldova) indicates correlation with the Unitary Association Zones 9–11 of the biozonation of [Baumgartner *et al.* \(1995\)](#) and with the mid- to late Oxfordian to late Kimmeridgian/early Tithonian interval. In addition, the co-occurrence of these two species (*Z. ovum* and *F. sphaerica*) with *Cinguloturris carpatica* (Dumitrica) indicates that the studied radiolarian assemblage also correlates with Unitary Association Zones B–D of [Beccaro \(2004\)](#), which corresponds to a mid-(?) to late Oxfordian to early Kimmeridgian interval.

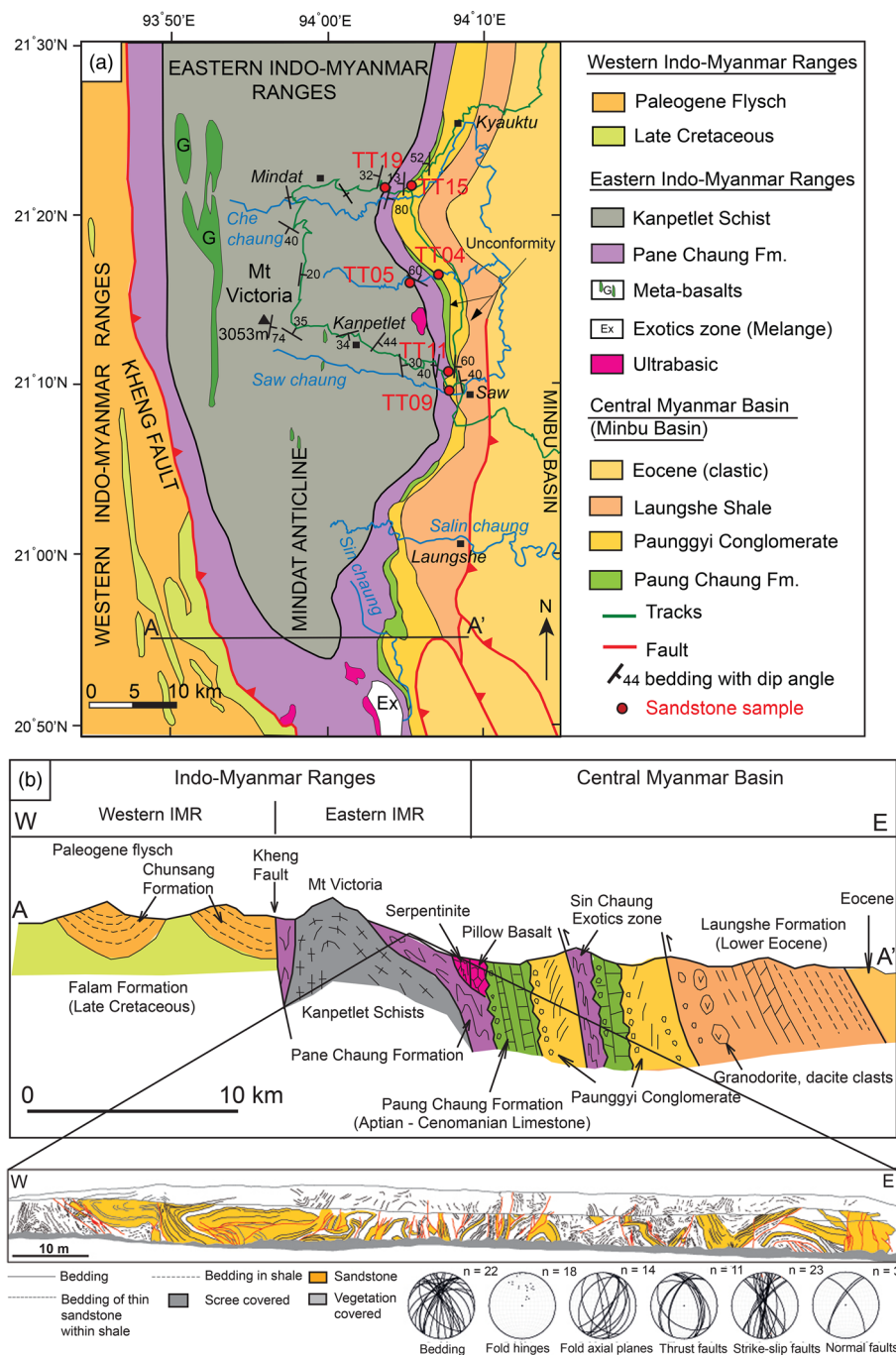


Fig. 4. (a) Outline geological map of the Mt Victoria area showing the broadscale distribution of the geological units and sample locations. (b) Geological cross-section across the Mt Victoria belt. See Figure 3a for location. Source: part (a) modified from United Nations (1979) and Mitchell *et al.* (2010); part (b) modified after Mitchell (1993) and Searle *et al.* (2017).

Petrography

Six sandstone samples mapped as Triassic from the core of the IMR (KM04, KM23, KM25, KM38, KM76a and TT19), eight samples from the Inner Belt (IBR10, IBR45a, IBR101, KM15, KM34, KM34a, KM54b and KM60) and six samples from the CMB (TT04, TT09, TT11, TT15 and KM40a, b) were analysed to understand better the general petrography and provenance of the IMR and CMB.

All the sandstones in this study were plotted on the ternary diagrams of Dickinson (1985), Garzanti (2016), and Garzanti (2019) (Fig. 8). All the analysed samples from the core of the IMR are litho-quartzose and feldspatho-litho-quartzose (Fig. 8a), composed predominantly of angular to subrounded monocrystalline quartz with subordinate polycrystalline quartz, plagioclase and lithic fragments, including phyllite, mudstone, chert and intermediate to basic volcanic rocks (Table 1) (Fig. 9a). Monocrystalline quartz grains constitute 37–56% of the total framework grains.

Lithic fragments constitute 9–41% of the framework grains. Some plagioclases have been partly altered to clays and clay cement has formed around the detrital grains. Muscovite, biotite, chlorite and heavy minerals are present in all samples (Table 1). The locally pore-filling matrix in all sandstones is dominated by clay minerals, authigenic cement (siderite, calcite and pyrite) and organic matter. Texturally, the sandstones are immature and poorly to moderately sorted. The Upper Triassic sandstones lie within the recycled orogenic province on quartz, feldspar, lithics (QFL) ternary diagrams (Garzanti 2019) (Fig. 8b).

Petrographic examination of the sandstone samples from the Inner Belt reveals that they are feldspatho-quartzo-lithic and quartzo-lithic (Fig. 8a), composed predominantly of monocrystalline quartz with subordinate polycrystalline quartz and lithic fragments. The lithic fragments include volcanic detritus (felsic) with subordinate sedimentary (argillaceous) and metamorphic (phyllitic) fragments (Fig. 9b). Lithic fragments constitute 46–67% (IBR10, IBR45a, IBR101, KM15 and KM60) of the total

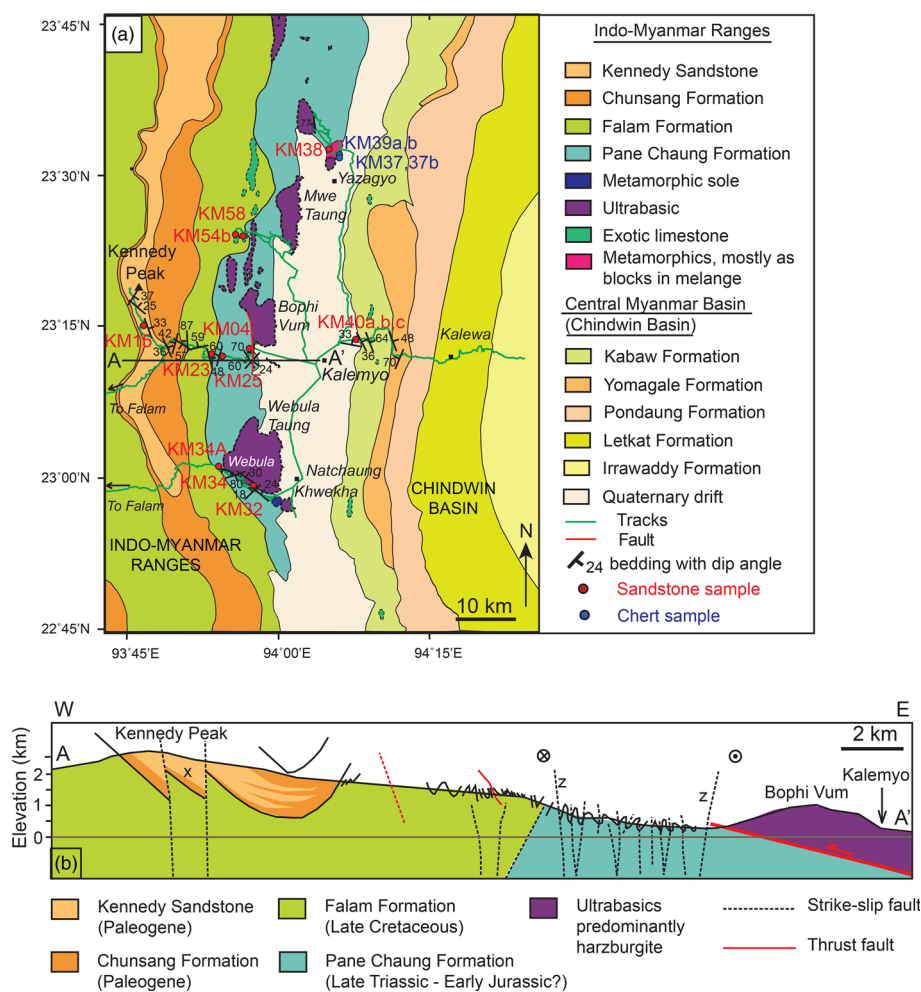


Fig. 5. (a) Outline geological map of the Kalemmyo area showing the broadscale distribution of the geological units and sample locations. (b) Geological cross-section along the Kalemmyo–Falam road based on field observations. ‘z’ represent hypothetical strike-slip faults driving uplift of Pane Chaung Formation. Strike-slip faults observed in the field that affect the Kennedy Peak Sandstone are schematically shown around location X. The presence of these faults minimizes the westwards thickening of the Chunsang Formation. See Figure 3a for location. Source: part (a) modified from United Nations (1979) and Mitchell *et al.* (2010); part (b) modified after Morley *et al.* (2020).

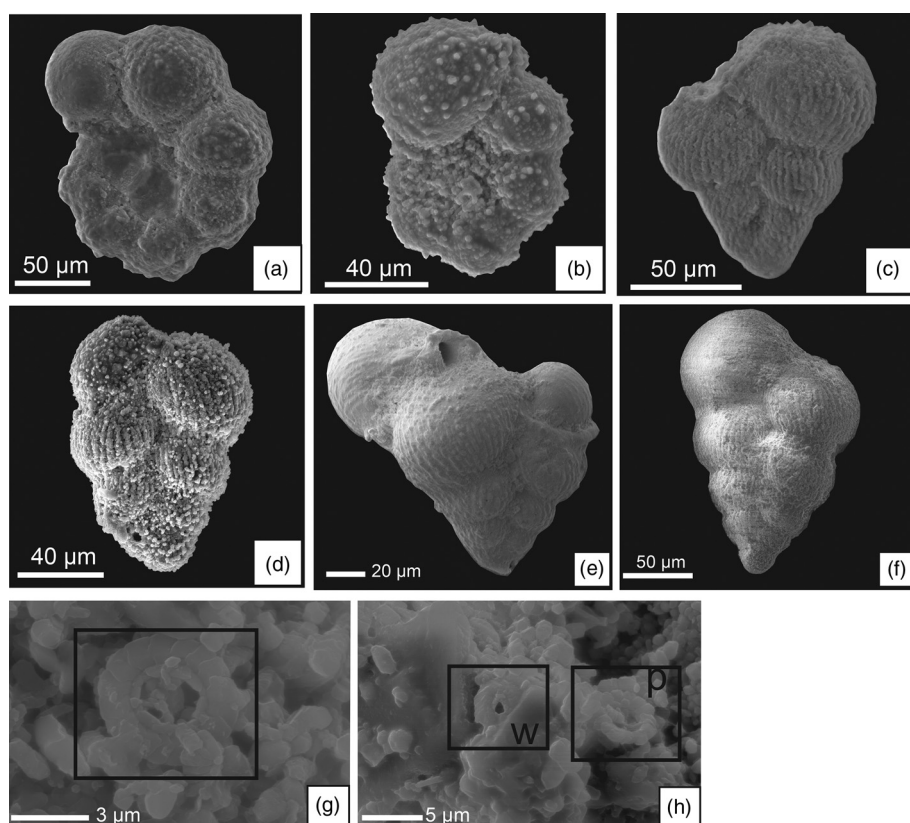


Fig. 6. Scanning electron microscopy images of microfossils and nannofossils from the Padaung–Taungup road section. (a) *Planohedbergella ultramicra* (Subbotina) (sample IBR108). (b) *Muricohedbergella planispira* (Tappan) (sample IBR103). (c) *Planoheterohelix globulosa* (Ehrenberg) (sample IBR108). (d) *Planoheterohelix globulosa* (Ehrenberg) (sample IBR98). (e) *Chiloguembelina wilcoxensis* (Cushman & Ponton) (sample IBR06). (f) *Chiloguembelina ototara* (Finlay) (sample IBR12). (g) *Prediscosphaera columnata* (Stover) (sample IBR103). (h) p, *Prediscosphaera columnata* (Stover) and w, *Watznaueria* sp (sample IBR103).

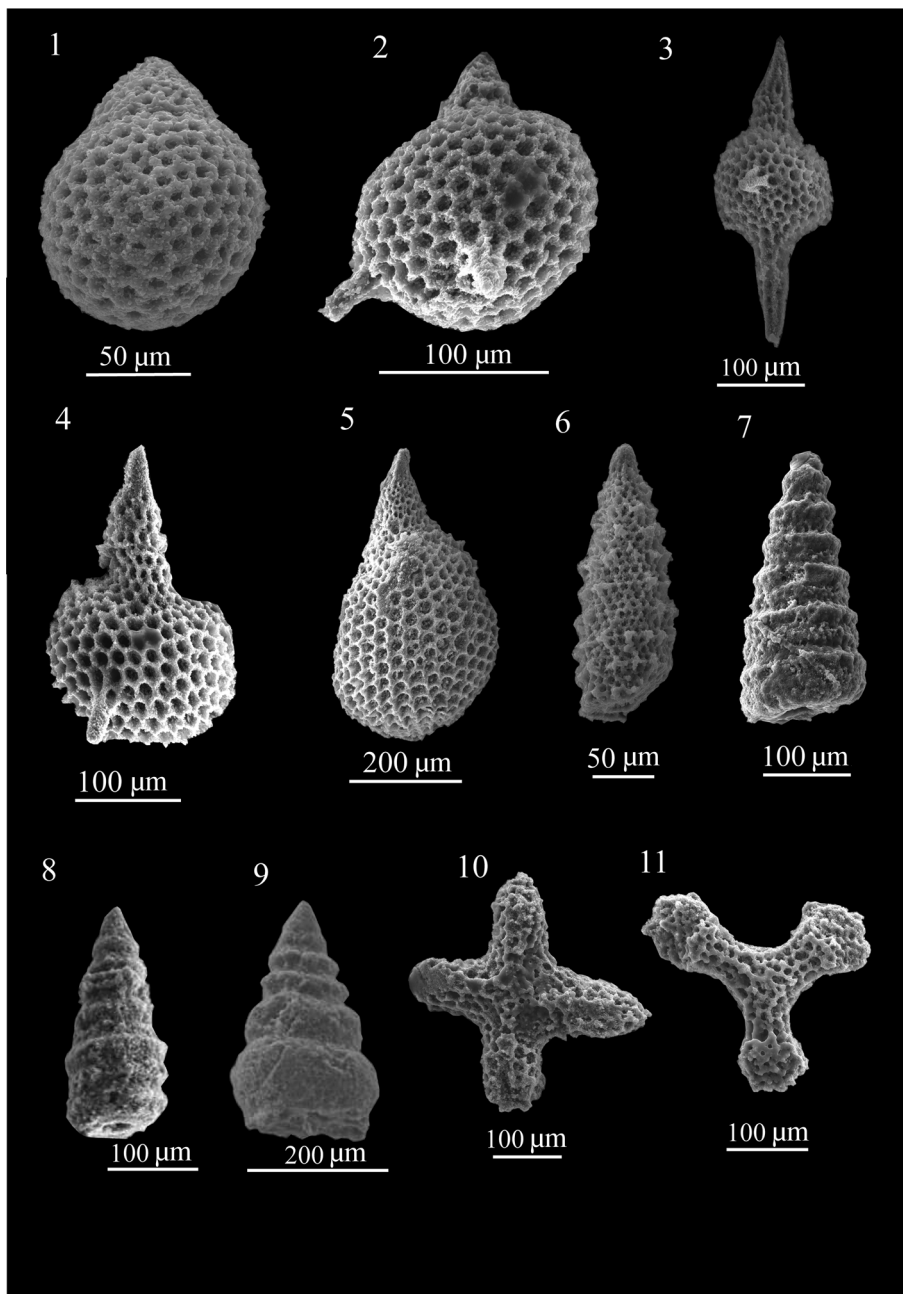


Fig. 7. Scanning electron microscopy images of radiolarians from a radiolarian chert (sample KM37b) associated with the Kalemmyo Ophiolite. 1, *Zhamoidellum ovum* (Dumitrica). 2, *Fultacapsa sphaerica* (Ozoldova). 3, 4, *Podobursa triacantha* (Fischli). 5, *Olanda* sp. 6, *Eoxitus dhimenaensis* (Baumgartner). 7, 8, *Cinguloturris carpatica* (Dumitrica). 9, *Cinguloturris latiannulata* (Grill and Kozur). 10, *Higumastra* sp. 11, ? *Angulobracchia biordinalis* (Ozoldova).

framework grains (Fig. 9c, d). On a QFL plot, the Eocene sandstones lie within the magmatic arc province (Table 1, Fig. 8b). Angular to subrounded, poorly sorted monocrystalline quartz grains constitute 23–46% (KM34, KM34a and KM54b) of the total framework grains and the sandstones lie within the recycled orogenic province on the QFL diagram (Table 1, Fig. 8b). On the LmLvLs plot, sandstones from the IMR are distributed in the magmatic arc field (Fig. 8c) (Garzanti 2019). Feldspar is dominated by plagioclase that exhibits euhedral crystal outlines and well-developed twinning. The matrix content is high in these mineralogically and texturally immature sandstones.

Detrital zircon U–Pb ages

Six sandstone samples (KM23, KM25, KM32, KM76a, TT05 and TT19) from the Pane Chaung Formation in the core of the IMR yielded >100 concordant zircon U–Pb ages (Fig. 10). Detrital zircon U–Pb ages range from 3474 ± 37 to 211 ± 9 Ma. The age distributions are consistent with three main clusters in the

Mesoproterozoic (1.25–1.0 Ga, 17% of the total analysed grains), Neoproterozoic–Cambrian (750–490 Ma, 31%) and Late Paleozoic–Early Mesozoic (350–210 Ma, 29%) and scattered Paleoproterozoic–Archean (3.4–1.6 Ga) and Ordovician–Devonian (480–370 Ma) ages. The youngest zircon is 211 ± 9 Ma and the weighted average ages range from 235 ± 2 to 221 ± 2 Ma (Fig. 10).

Twelve samples from the thick Mesozoic–Cenozoic flysch unit in the Inner Belt of the IMR were analysed. Of these, six samples (KM34, KM34a, KM54b, KM58, IBR102 and IBR110A) are from outcrops mapped previously as Cretaceous and six (IBR01, IBR11, IBR48A, IBR71B, KM15 and KM60) as Paleogene, based on fossil evidence (Bender 1983) and geological maps (United Nations 1979; Soe *et al.* 2014). A total of 445 zircons were analysed from the Falam Formation near Kalemmyo (KM34, KM34a, KM54b and KM58), yielding 354 concordant zircon ages. The zircon age spectra from all samples display a prominent age peak at 120–80 Ma and scattered Proterozoic, Paleozoic and Mesozoic ages (Fig. 11). The youngest ages are 82–67 Ma with a weighted average age of 74 ± 1 Ma (MSWD = 0.23, $n = 3$) (Fig. 11). A total of 221 zircon grains

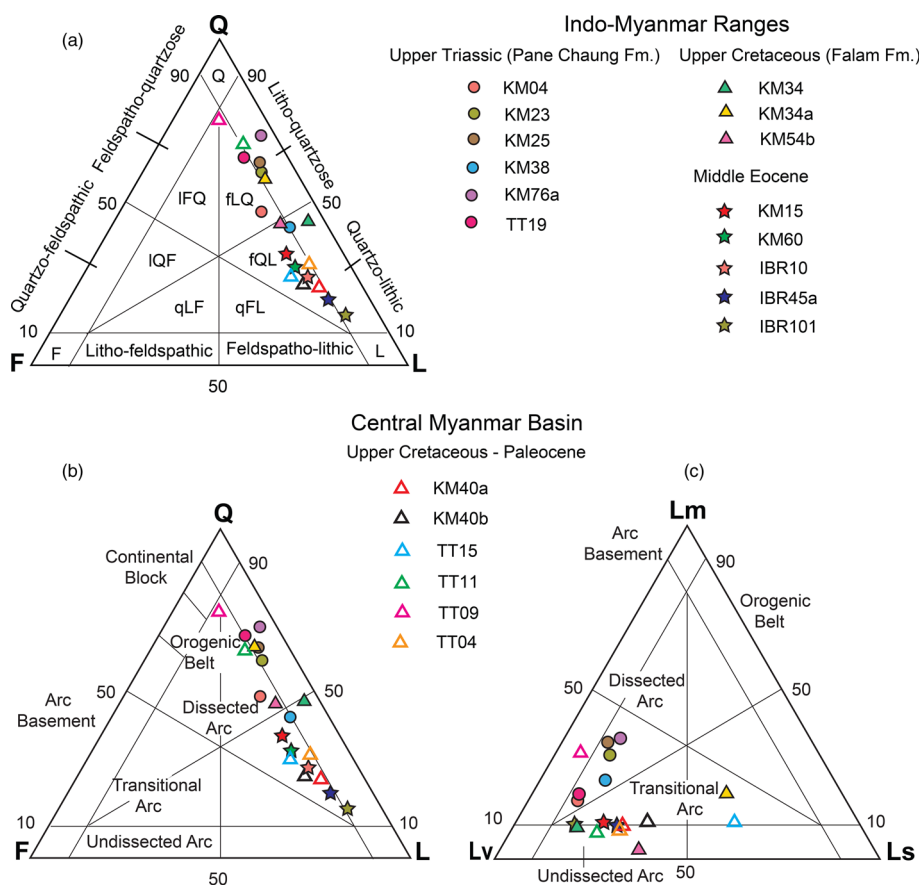


Fig. 8. QFL and LmLvLs plots of the Indo-Myanmar Ranges and Central Myanmar Basin sandstones. **(a)** Sandstone classification. **(b)** Provenance and **(c)** LmLvLs fields. QFL, quartz, feldspar, lithic fragments; Lm, metamorphic; Lv, volcanic; Ls, sedimentary; Q, quartzose; F, feldspathic; L, lithic; IFQ, litho-feldspatho-quartzose; fLQ, feldspatho-litho-quartzose; IQF, litho-quartzo-feldspathic; fQL, feldspatho-quartzo-lithic; qLF, quartzo-litho-feldspathic; qFL, quartzo-feldspatho-lithic. Source: Part (a) after Garzanti (2016); parts (b, c) after Dickinson (1985) and Garzanti (2019).

were analysed from the samples previously mapped as Cretaceous along the Padaung–Taungup road section in the more southerly IMR in Rakhine (IBR102 and IBR110A). These analyses yielded 214 concordant zircon ages that ranged from 1734 ± 17 to 43 ± 1 Ma. The samples exhibit a prominent Cretaceous cluster at 110–80 Ma, with a subordinate cluster at c. 50 Ma, as well as scattered Triassic and Precambrian ages (Fig. 11).

A total of 396 zircon grains were analysed from samples mapped previously as Paleogene along the Padaung–Taungup road section (IBR01, IBR11, IBR48A, IBR71B and KM60) and one sample (KM15) from the Eocene Kennedy Sandstone, west of Kalemmyo. The Padaung–Taungup road samples yielded 327 concordant zircon ages with 118 concordant ages from KM15. Detrital zircon U–Pb ages from the Paleogene samples ranged from 2759 ± 20 to 43 ± 2 Ma. They contain abundant Cretaceous (65–71%), Eocene (7–18%), Paleocene (3–6.5%), as well as some Jurassic, Triassic, Permian and Precambrian ages (Fig. 12). IBR48A contains an abundant Paleocene (21%) population, but yielded no Eocene grains. The zircon age spectra from all samples display a prominent age peak at 120–80 Ma. Cretaceous zircons are predominantly euhedral and subhedral. They exhibit a simple oscillatory growth pattern on cathodoluminescence images, suggesting a contemporaneous igneous provenance.

Detrital zircon Hf isotopes

Six samples (KM15, KM34, KM34a, KM54b, IBR71B and IBR102) from the Inner Belt of the IMR were selected for Hf isotope analysis using the same zircon grains measured for U–Pb. The ϵHf values are predominantly positive for both the Cretaceous and Eocene samples, ranging from +0.5 to +17 (Fig. 13a, b). A few grains have negative values ranging from 31 to –1. The majority of the ϵHf values are located between the depleted mantle and chondritic lines, with a few grains below the chondritic line.

Discussion

Depositional environments and refinements of IMR regional stratigraphy

Triassic flysch

The United Nations (1979) mapping project identified Triassic flysch exposed in the IMR. The Triassic age of the Pane Chaung Formation is based on the rare occurrence of *Halobia* fossils (Gramann 1974; United Nations 1979; Bannert *et al.* 2011; Yao *et al.* 2017; J.E. Zhang *et al.* 2017) and detrital zircon U–Pb dating (Sevastjanova *et al.* 2016; Yao *et al.* 2017; this study). In the southern IMR, along the Gwa road section, ultramafic rocks are thrust over sediments (J. Zhang *et al.* 2018, their fig. 13) that are of either Triassic (Pane Chaung Formation; United Nations 1979, p. 32, their fig. 20) or Eocene (J. Zhang *et al.* 2018; their fig. 11c) age. Detrital zircons from a flysch sample (KM76a) collected in close proximity to the eastern margin of the ultramafic rocks at this locality have an age profile similar to other Pane Chaung Formation samples and are considered to be Triassic, supporting the interpretations of the United Nations (1979). We also consider it likely that the western margin of the ultramafic rocks is thrust over Triassic sediments (United Nations 1979, their fig. 20), although, a few kilometres further west, J. Zhang *et al.* (2018) reported Eocene plant fossils and detrital zircons, so it is possible that Eocene sediments are also present in some areas along this boundary. The discontinuous nature of the ultramafic rocks and Triassic sediments in the IMR leads to considerable uncertainty in mapping the extent of the Pane Chuang Formation, but detrital zircon analysis provides a clear path forward to reconstructing the occurrence and extent of the Triassic flysch.

Jurassic–Early Cretaceous deposition

The abundant and well-preserved Upper Jurassic radiolarians from chert associated with the Kalemmyo Ophiolite provide age constraints

Table 1. Detrital modes of samples analysed from the Indo-Myanmar Ranges

Sample No.	Quartz			Feldspars			Lithics/rock fragments								Authigenic minerals and matrix Quartz + plagioclase + calcite cement	Heavy minerals and opaques
	Monocrystalline quartz	Polycrystalline quartz	Total quartz	Plagioclase feldspar	K-feldspar	Total feldspar	Sedimentary lithic	Metamorphic lithic	Volcanic lithic	Chert	Muscovite	Biotite	Chlorite	Total lithics/rock fragments		
IBR10	14.5	8.0	22.5	10.5	0.0	10.5	14.2	4.2	31.0	0.0	1.4	0.0	0.0	50.8	13.8	2.4
IBR45a	12.0	5.4	17.4	9.8	0.0	9.8	15.4	5.8	35.8	0.0	0.0	0.6	1.6	59.2	13.2	0.4
IBR101	9.8	3.2	13.0	8.0	0.0	8.0	10.8	7.0	49.0	0.0	0.4	0.2	0.0	67.4	10.8	0.8
TT04	25.8	4.0	29.8	10.0	0.0	10.0	16.0	4.8	35.0	0.0	0.0	0.0	0.0	55.8	4.0	0.4
TT09	42.0	10.0	52.0	9.0	0.0	9.0	0.6	2.5	5.0	0.3	0.3	0.2	0.0	8.9	30.0	0.1
TT11	33.7	9.0	42.7	8.0	0.0	8.0	3.0	1.0	9.0	0.0	1.0	1.5	1.0	16.5	32.5	0.3
TT15	20.0	5.0	25.0	15.0	0.0	15.0	25.0	5.0	15.0	1.0	0.0	1.0	1.0	48.0	12.0	0.0
TT19	41.5	8.0	49.5	7.0	0.0	7.0	2.0	3.0	11.0	0.0	0.2	0.3	0.0	16.5	27.0	0.0
KM04	25.8	14.0	39.8	12.6		12.6	3.8	5.0	20.0	2.2	1.2		0.2	32.4	15.0	0.2
KM15	17.0	11.0	28.0	12.0		12.0	8.4	4.0	24.0	3.0	1.2	1.0	0.6	42.2	15.8	2.0
KM23	41.0	9.0	50.0	7.4		7.4	2.8	5.6	10.0	1.2	4.2	2.6	0.6	27.0	13.6	2.0
KM25	40.5	10.2	50.7	6.8		6.8	2.2	6.0	9.3	1.2	3.2	1.2	0.8	23.9	17.1	1.5
KM34	15.0	8.0	23.0	2.0		2.0	4.2	2.4	18.0	2.0		0.2	0.2	27.0	46.6	1.4
KM34a	34.0	12.4	46.4	6.6	0.2	6.8	9.8	3.8	6.0	5.2			2.0	26.8	19.6	0.4
KM38	27.6	9.2	36.8	8.4		8.4	5.6	7.2	19.0	0.8	1.0	7.2	0.6	41.4	12.6	0.8
KM40a	13.5	7.0	20.5	9.5	0.2	9.7	15.0	5.0	32.0	2.4			0.8	55.2	13.2	1.4
KM40b	14.5	7.0	21.5	12.6	0.4	13.0	16.0	5.0	25.5	4.8				51.3	13.4	0.8
KM54b	25.8	4.8	30.6	8.5		8.5	10.4	1.0	17.5	3.0				31.9	27.8	1.2
KM60	20.4	5.6	26.0	13.0	0.0	13.0	12.5	5.8	23.4	2.0	1.6	0.2	1.2	46.7	14.1	0.2
KM76a	29.8	26.2	56.0	3.2	0.0	3.2	3.2	7.6	11.0	0.4	0.2	0.0	0.6	23.0	17.4	0.4

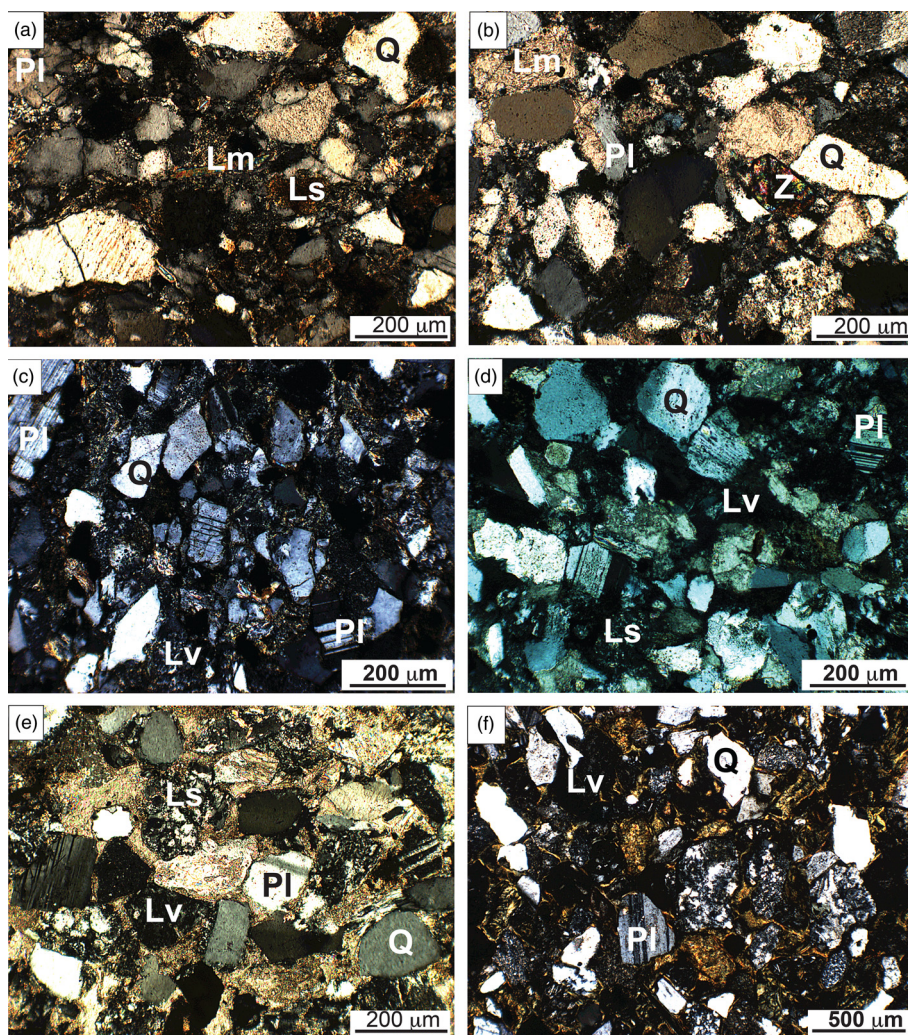


Fig. 9. Photomicrographs of sandstones. (a) Pane Chaung Formation, Indo-Myanmar Ranges. (b) Falam Formation, Indo-Myanmar Ranges. (c, d) Eocene sandstones, Indo-Myanmar Ranges. (e, f) Kabaw Formation, Central Myanmar Basin. Lm, metamorphic lithic; Ls, sedimentary lithic; Lv, volcanic lithic; Pl, plagioclase; Q, quartz; Z, zircon.

on the timing of deep-marine sedimentation in this portion of the Naga–Andaman suture zone (Fig. 7). Based on the radiolaria, chert sample KM37b was probably deposited during the mid- to late Oxfordian to late Kimmeridgian/early Tithonian interval. The age of this chert sample from the Kalemmyo Ophiolite is broadly consistent with previous biostratigraphic results from the same area that yielded a Jurassic–Cretaceous radiolarian fauna with a likely Mid-Jurassic age (J. Zhang *et al.* 2018). Reworked chert pebbles of Callovian–Kimmeridgian age in the Pondaung Formation in the CMB have been inferred to have been derived from the Kalemmyo Ophiolite (Suzuki *et al.* 2004) and are consistent with the biostratigraphic ages reported here and in J. Zhang *et al.* (2018). A Mid- to Late Jurassic age for the cherts is also consistent with radiometric dating (U–Pb ages and K–Ar ages) of the Kalemmyo Ophiolite, which suggests an Early Cretaceous age for the ophiolite itself (Mitchell 1981; Liu *et al.* 2016b; J. Zhang *et al.* 2018). Importantly, these biostratigraphic and radiometric results from the Kalemmyo Ophiolite are comparable with temporal constraints of deep-marine sedimentation from the Nagaland Ophiolite (e.g. Sarkar *et al.* 1996; Baxter *et al.* 2011; Aitchison *et al.* 2019) and ophiolites in Tibet (e.g. the Xialu, Zedong and Zhongba ophiolites) (Matsuoka *et al.* 2002; Aitchison *et al.* 2007; Li *et al.* 2013). These results are therefore consistent with the hypothesis that the Kalemmyo, Nagaland and IYTSZ ophiolites were once part of the same Neotethyan ocean floor (Fig. 14a, b).

Jurassic–Lower Cretaceous sediments are only demonstrably known from the radiolarian cherts associated with the Nagaland–Manipur and Kalemmyo ophiolites (Baxter *et al.* 2011; J. Zhang *et al.* 2018; Aitchison *et al.* 2019). Other than these occurrences, there

appears to be an almost total absence of Jurassic–Lower Cretaceous sedimentary rocks in the IMR (Bannert *et al.* 2011), although this might be due to a lack of fossiliferous sediments. Recently published detrital zircon analyses from the Pane Chaung Formation indicate that the maximum depositional ages are predominantly Late Triassic, together with some Early Jurassic ages for a small number of grains (Sevastjanova *et al.* 2016; Yao *et al.* 2017). Hence the upper portions of the Pane Chaung Formation extend into the Lower Jurassic. Khin *et al.* (2022) interpreted the presence of Jurassic greywackes in the IMR, but their extrapolation does not seem to be supported by detrital zircon or biostratigraphic ages, for which further work is required. Although Early Cretaceous age zircons are present in the Upper Cretaceous Falam Formation, it has not been possible to identify any Lower Cretaceous clastic sediments in the IMR.

Paleogene deposition

The rarity of Cretaceous–Paleogene planktonic forams suggests that microfossils are generally diluted by the clastic input in the IMR ‘flysch’ facies. Also, some degree of post-depositional removal presumably took place via diagenesis/dissolution. Three mudstone samples mapped as Cretaceous (IBR98, IBR103 and IBR108) contain Cretaceous planktonic forams, although detrital zircon U–Pb dating of sandstone samples (IBR102 and IBR110A) in the same unit yields Paleogene detrital zircons, with the youngest population indicating the assignment of a Lutetian (or younger) depositional age. This suggests that either the Cretaceous planktonic forams were reworked into younger sediments, or that some unrecognized

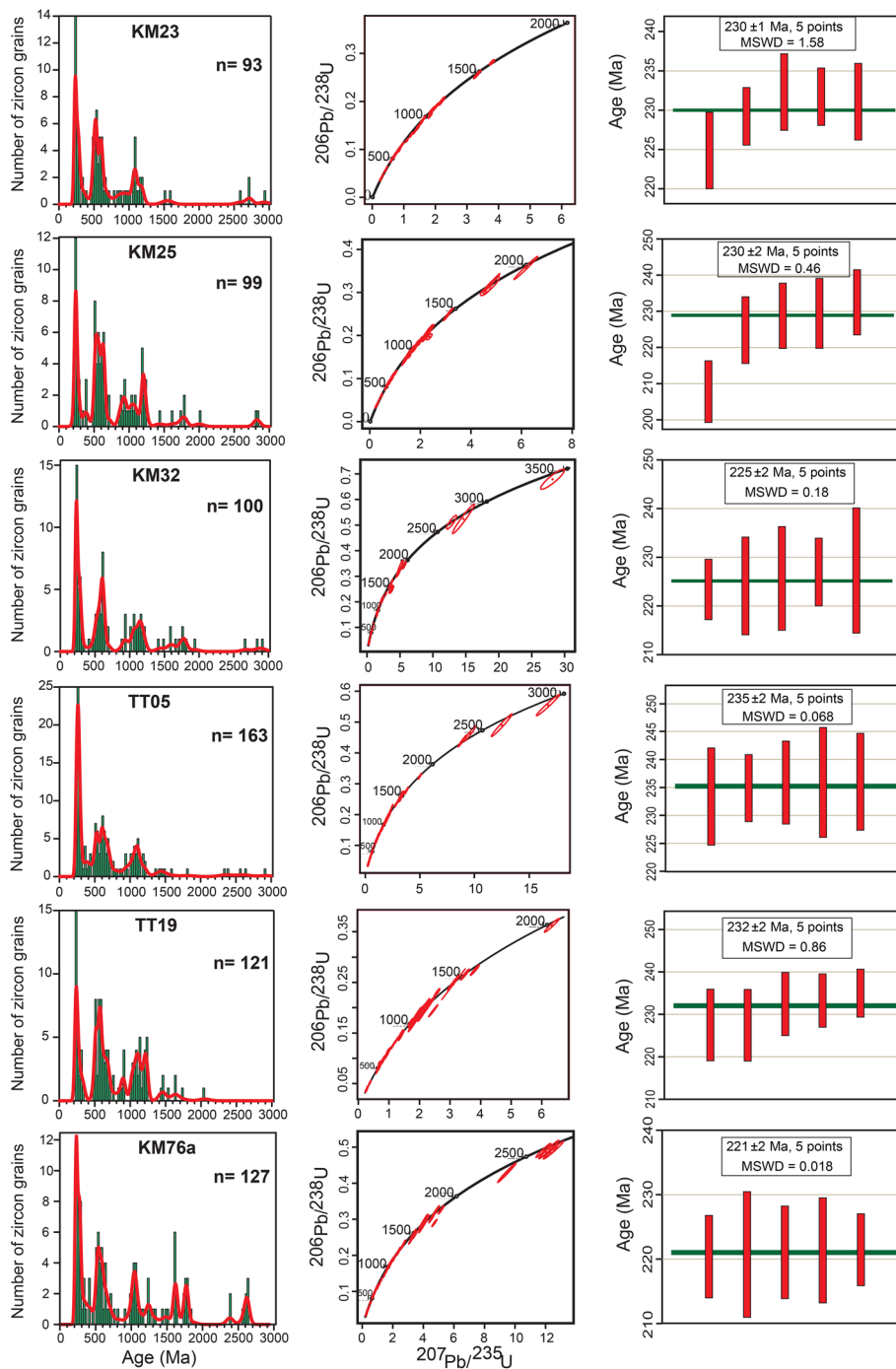


Fig. 10. Histograms and kernel density plots, concordia diagrams and weighted average age diagrams showing detrital zircon U–Pb ages of the Pane Chaung Formation.

structural complexity exists that juxtaposes Cretaceous fossil-bearing strata with the Eocene units. We favour the first hypothesis given that previous workers have also noted the allochthonous nature of some of the Cretaceous outcrops and the reworking of some Cretaceous fossils into Cenozoic units (Gramann 1974; Bender 1983). Brunnschweiler (1966) suggested that the bulk of the flysch is not older than Eocene based on the youngest fossils known at that point. In contrast with the samples mapped as Cretaceous, the Paleogene sandstones yield youngest zircon age populations that are consistent with their mapped age.

Flysch source terranes

Upper Triassic provenance

Sandstone compositions in the Pane Chaung Formation indicate a recycled orogenic provenance. This is further supported by a broad spread of the zircon U–Pb age distribution in sandstones, indicating

contributions from multiple sources. This is also diagnostic of mixed provenance and reworking. The Upper Paleozoic–Lower Mesozoic Pane Chaung zircon grains have euhedral to subhedral morphologies and well-developed oscillatory compositional zoning, suggesting a contemporaneous volcanic provenance. The Upper Paleozoic–Lower Mesozoic zircons have a wide range of ages from *c.* 300 to 200 Ma and ϵ_{Hf} values from -6 to $+11$ (Yao *et al.* 2017), suggesting a magma contribution from a juvenile source. The youngest zircon grains approximate the depositional age of the samples, which confirms the existence of contemporaneous volcanic activity, corroborated by abundant mafic to intermediate volcanic lithic fragments and plagioclase. The combination of evidence from Upper Triassic sandstones indicates a long-lived magmatic arc source.

Four models have been proposed to explain the source terrane for the Pane Chaung Formation. In model A, West Myanmar was part of the Sibumasu Terrane, or a neighbouring terrane, during the

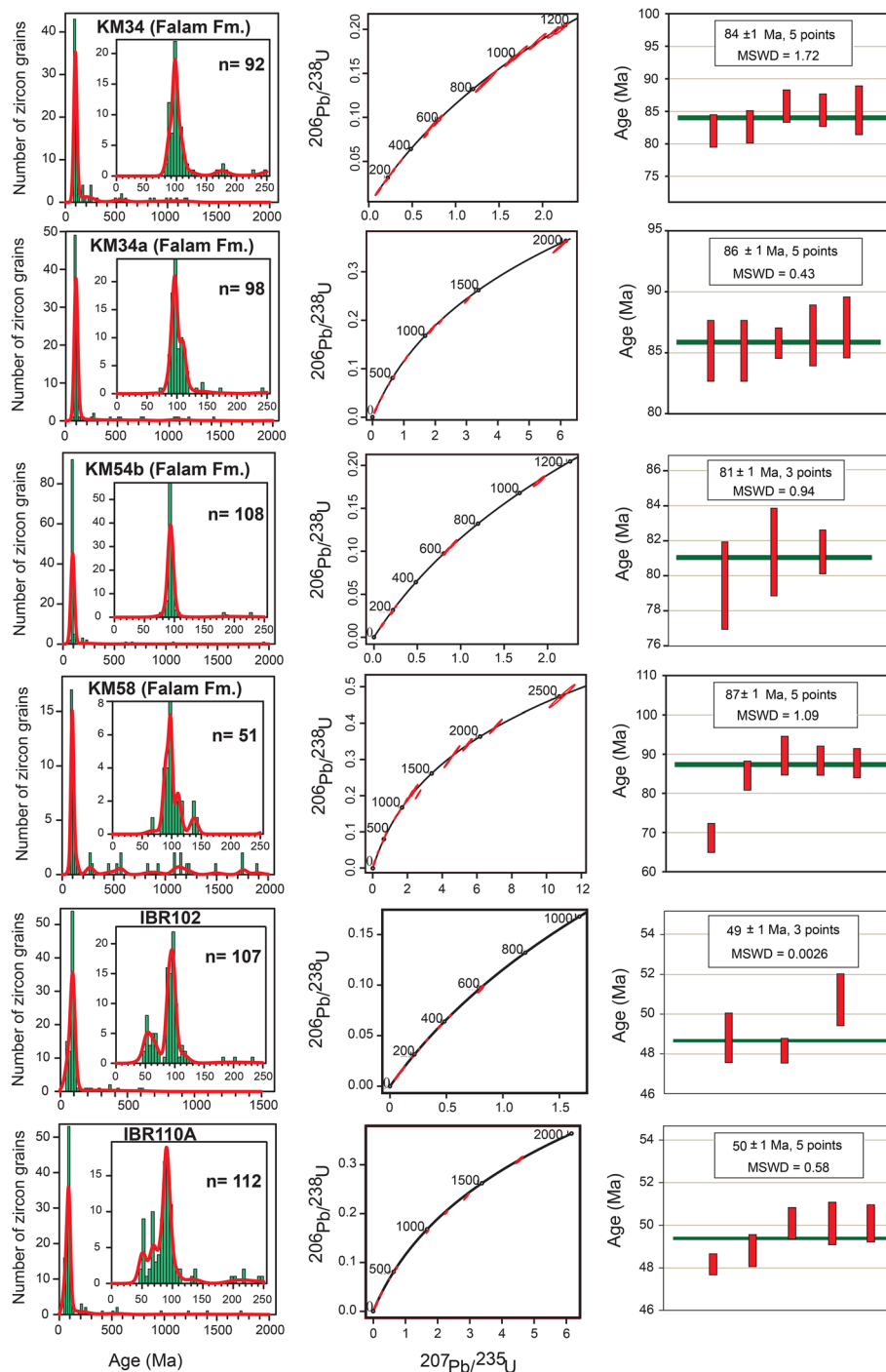


Fig. 11. Histograms and kernel density plots, concordia diagrams and weighted average age diagrams showing detrital zircon U–Pb ages of the Falam Formation and Padaung–Taungup road section.

Triassic (Sevastjanova *et al.* 2016; J. Zhang *et al.* 2018). In model B, West Myanmar lay adjacent to the future northeastern part of India in northern Gondwana and received sedimentary detritus from sources to the south (Wang *et al.* 2016). In model C, West Myanmar lay adjacent to the future northeastern part of India in northern Gondwana and received sediment derived from the future eastern Australia plate to the east (Cai *et al.* 2016; Yao *et al.* 2017; Fang *et al.* 2018). In model D, West Myanmar received sediment sourced from the future eastern Australian plate and rifted from the northern Australian margin at a location attributed to Argoland (X. Zhang *et al.* 2021). These models imply three significantly different scenarios for the tectonic position of the WMT and its subsequent evolution and will be discussed individually. In order to assess these models, published U–Pb and Hf isotopic analyses for detrital zircons in the age-equivalent sandstones of the Sibumasu Terrane, Lhasa Terrane, NW Australia and the Langjiexue Formation of

southern Tibet are reviewed and compared with new and published data from the Upper Triassic Pane Chaung Formation (Fig. 15).

In model A (Sevastjanova *et al.* 2016), the Upper Triassic Pane Chaung Formation was part of SE Asia prior to the Indosinian Orogeny, with perhaps a close affinity to the Sibumasu sandstones. In this view, the Pane Chaung Formation cannot be associated with the Indian plate. However, the age spectra of detrital zircons from Upper Triassic–Lower Jurassic sandstones exposed in the Loi-an Group (or Shweminbon Group) of the Sibumasu Terrane (Cai *et al.* 2017) are significantly different from those from the Pane Chaung Formation (Fig. 15). Both units contain Triassic zircons, but, as discussed in Morley *et al.* (2020), key peaks in the Pane Chaung Formation occur at *c.* 700–500 and 1200–1000 Ma, correlating with troughs in the Loi-an Group. Similarly, although peaks for the Loi-an Group occur at *c.* 500–400, 900–700 and 1900–1800 Ma, these time intervals are represented by troughs in the Pane Chaung

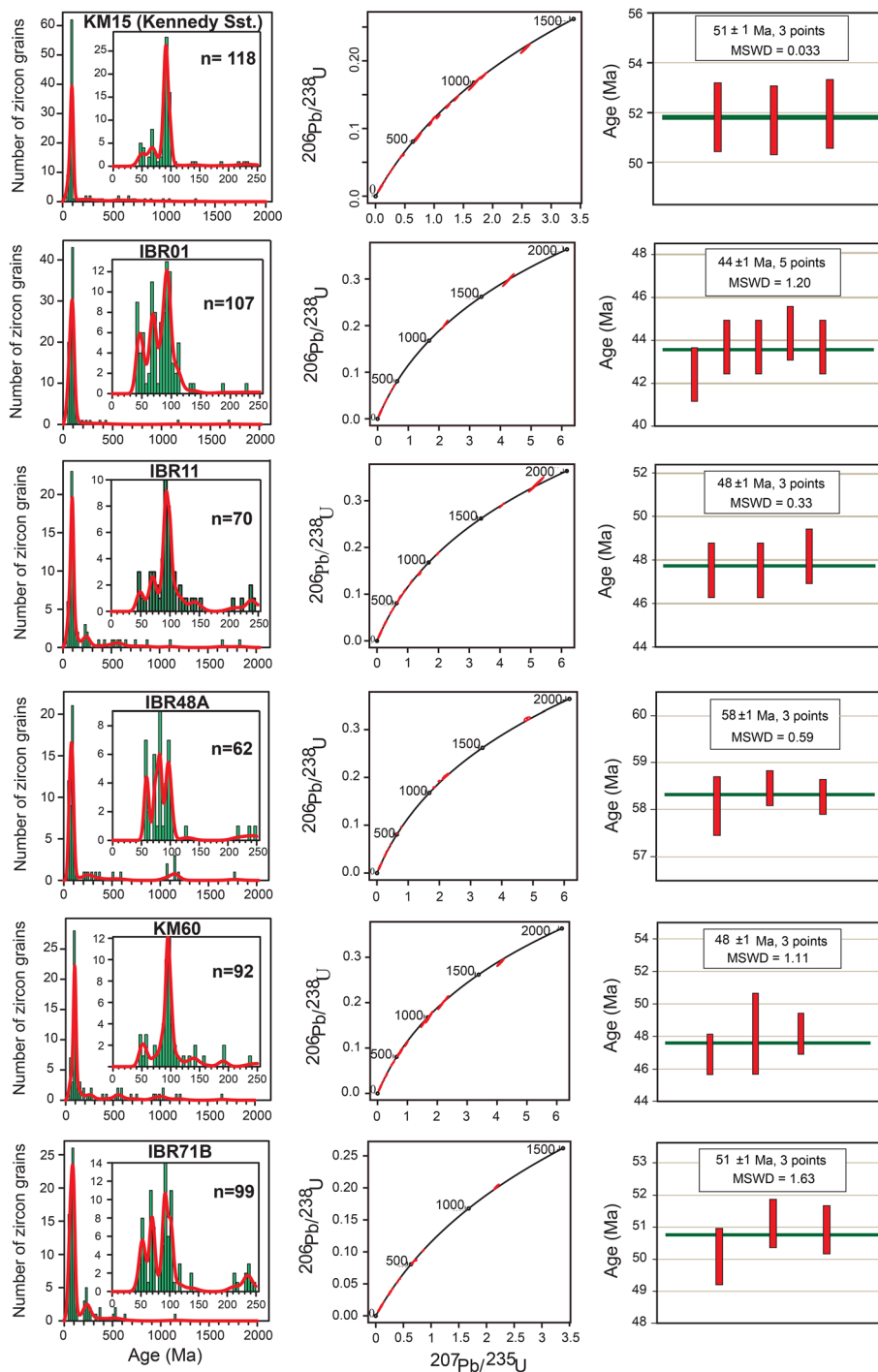


Fig. 12. Histograms and kernel density plots, concordia diagrams and weighted average age diagrams showing detrital zircon U–Pb ages of the Kennedy Sandstone and Padaung–Taungup road section.

Formation (Sevastjanova *et al.* 2016; Cai *et al.* 2017; Yao *et al.* 2017; this study). This suggests that the Pane Chaung and Sibumasu terranes were not derived from the same source area. However, to be more certain of this conclusion, a broader spectrum of samples from the Loi-an Group needs to be analysed. A further issue is that an early position in SE Asia is unable to explain how the Lower Cretaceous amber deposits in the northern WMT preserve an extensive flora and fauna of Gondwana origin, which implies rifting of the WMT from Gondwana in the Early Cretaceous (Poinar 2019).

In model B (Wang *et al.* 2016), Upper Triassic turbidites of the Langjiexue Group, exposed south of the IYTSZ in southern Tibet, have a similar petrographic composition and biostratigraphy and yield broadly similar U–Pb age spectra for the detrital zircons (Fig. 15) and ϵ_{Hf} values (Yao *et al.* 2017) as the Pane Chaung Formation. Coupled U–Pb age and Hf isotopic signatures for detrital zircons in the Pane Chaung Formation differ from those of

Upper Triassic sandstones of the Sibumasu and Lhasa terranes, but instead are similar to the Langjiexue Group in the northern Tethys Himalaya. Palaeocurrent directions from the Langjiexue Group indicate WNW-directed sediment transport (Wang *et al.* 2016). Unfortunately, no reliable palaeocurrent data exists for the Pane Chaung Formation for comparison, nor could they be measured in the field. The Langjiexue Group was originally deposited along or adjacent to the northern passive continental margin of the future Indian continent region of northern Gondwana in a deep-water fan system (Wang *et al.* 2016), whereas the Pane Chaung Formation was derived from the eastern part of the system. A plausible sediment source was a distant Gondwanide Orogeny to the south generated by Pan-Pacific subduction beneath the southeastern margin of Gondwana, with the sediment-routing system from the east (Wang *et al.* 2016). This model implies that the Pane Chaung Formation was either

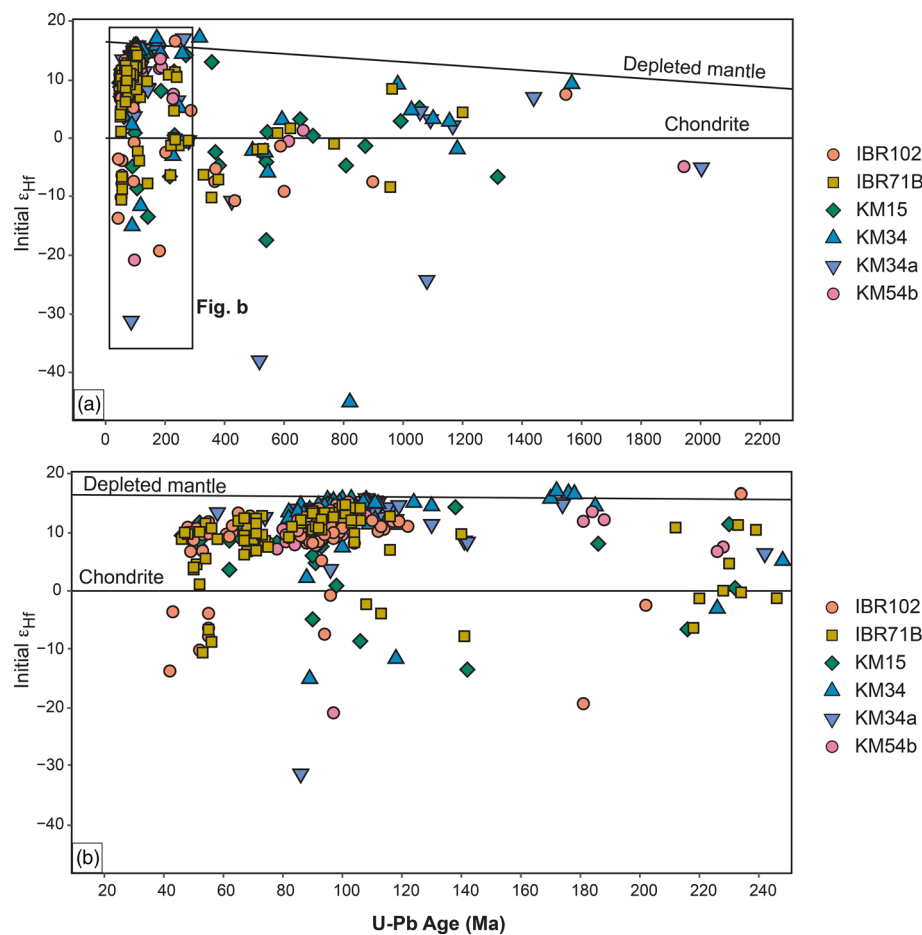


Fig. 13. Detrital zircon U–Pb v. $\epsilon_{Hf}(t)$ data for Upper Cretaceous–Paleogene samples from the Indo-Myanmar Ranges. (a) 0–2200 Ma ages. (b) 0–250 Ma ages; see part (a) for location.

part of the future NE Indian continental margin within northern Gondwana or adjacent to NE India.

In model C (Cai *et al.* 2016; Yao *et al.* 2017), the Pane Chaung Formation was deposited on a huge submarine fan extending from NW Australia to the continental margin of NE India on the northern margin of Gondwana. This scenario shows a location for the Pane Chaung Formation adjacent to NE India, similar to that proposed by Wang *et al.* (2016), but the sediment source area is different. In the

model of Cai *et al.* (2016) and Yao *et al.* (2017), the extent of the sedimentary system incorporating the Langjiexue Group is a vast region north of the future Australian plate on northern Gondwana, with the sediment sourced primarily from the ESE (including the Birds Head region).

Fang *et al.* (2018) proposed a similar source area, but their submarine fan was of much smaller extent (similar to Wang *et al.* 2016). The Langjiexue Group in this scenario lies at the SW limit of

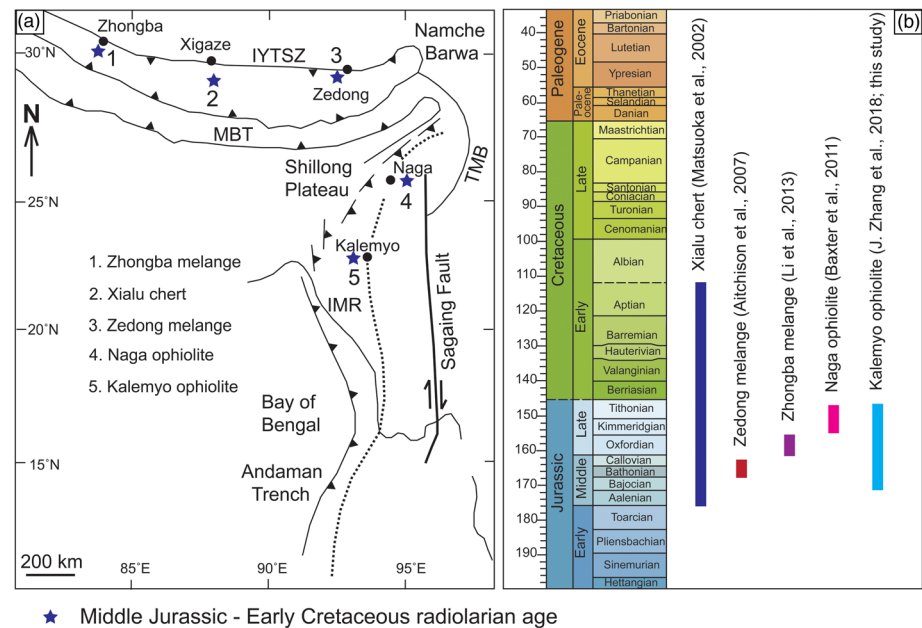


Fig. 14. (a) Map of the Himalayan and Myanmar regions showing the location of Indus–Yarlung Tsangpo suture zone and the Kalemmyo–Nagaland suture zone (dotted line between Naga and Kalemmyo). The highlighted numbers are five regions where radiolarians have been reported. (b) Chronostratigraphic chart summarizing the age constraints of deep-water sedimentation in the Neotethys Ocean. IMR, Indo-Myanmar Ranges; IYTSZ, Indus–Yarlung Tsangpo suture zone; MBT, Main Boundary Thrust; TMB, Tagaung-Myitkyina Belt. Source: part (a) modified after Baxter *et al.* (2011).

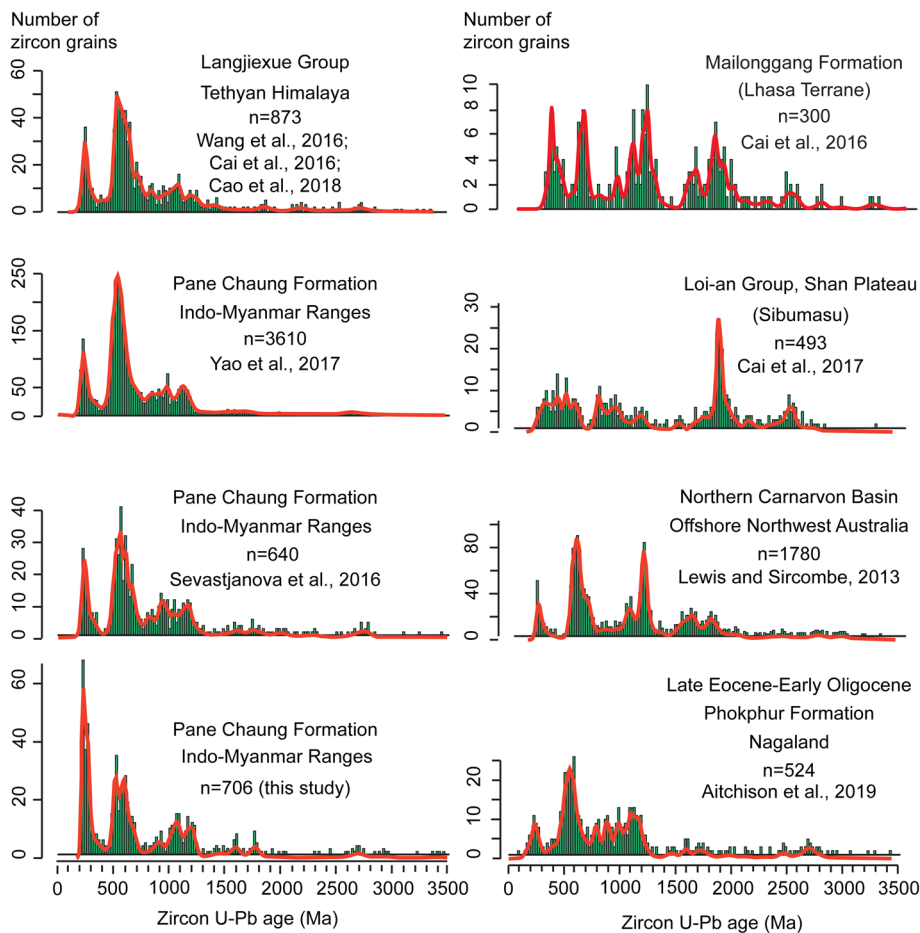


Fig. 15. Comparison of detrital zircon U–Pb data from the Pane Chaung Formation in the Indo-Myanmar Ranges (Sevastjanova *et al.* 2016; Yao *et al.* 2017; this study) with those from the Langjiexue Group (Cai *et al.* 2016; Wang *et al.* 2016; Cao *et al.* 2018), Nagaland (Aitchison *et al.* 2019), Sibumasu (Cai *et al.* 2017) and the Carnarvon Basin (Lewis and Sircombe 2013). All ages are displayed in 20 Ma bins (0–3500 Ma). Ordinate axis indicates the number of detrital zircon ages in each bin on the abscissa.

a fan on the future northern Greater India, whereas the Pane Chaung Formation lies just to the south. This scenario is based mainly on similar Permian–Triassic detrital zircon populations in the Pane Chaung Formation and age-equivalent rocks from the Bird’s Head region in western Papua and the Mungaroo Formation in the Carnarvon Basin on the NW shelf of Australia. However, in detail, there are several differences in the zircon age spectra (Wang *et al.* 2016). The Bird’s Head samples yielded ages dominantly between 280 and 200 Ma, with <15% Early Paleozoic–Precambrian ages (Gunawan 2012). A striking feature of the Pane Chaung sandstones is a large Permian–Triassic zircon population, but the Carnarvon Basin data show that these ages are only from a very small population of the total number of zircons (Lewis and Sircombe 2013). Zircons in the Carnarvon Basin display notable age clusters at 1250–1000 and 1850–1500 Ma that are rare in the Pane Chaung Formation. Cr-spinel is present in the Pane Chaung Formation, whereas Cr-spinel is rare in Western Australia (Sevastjanova *et al.* 2016).

In model D, West Myanmar is located on the northern Australian margin and is considered to represent a continental block that fits into the area from which Argoland is proposed to have rifted (X. Zhang *et al.* 2021). The sediment source area for the Pane Chaung Formation is similar to model C. The link with the Langjiexue Group is minimized, which is a potential weakness with this model.

The close affinity of the Pane Chaung Formation with the Langjiexue Group (models B and C) and palaeomagnetic data (Westerweel *et al.* 2019) support post-Triassic rifting of a continental (and oceanic?) terrane upon which the Pane Chaung Formation was deposited (Fig. 16). Furthermore, this fragment was probably bearing Gondwana flora and fauna, suggesting that rifting occurred in the Early Cretaceous (Poinar 2019). This terrane could be the Indian plate, the WMT or a small continental fragment (the Mt Victoria Block), which is postulated to have collided with the

WMT in the mid-Cretaceous (Mitchell 1993; see discussions in Morley *et al.* 2020; Licht *et al.* 2020). These different tectonic models are discussed further in the following sections.

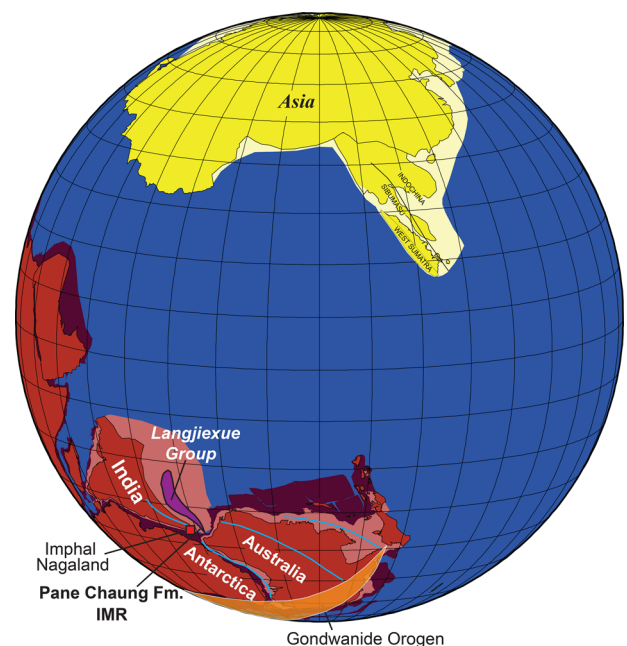


Fig. 16. Simplified Late Triassic palaeogeographical reconstruction illustrating our preferred scenario for the provenance and depositional setting of the Pane Chaung Formation. Source: plotted on a stereographic projection redrawn and modified from Sevastjanova *et al.* (2016), with additional information from Wang *et al.* (2016) and Aitchison *et al.* (2019).

Upper Cretaceous–Paleogene provenance

A broad similarity in the U–Pb zircon age distribution and Hf isotope compositions for Upper Cretaceous–Paleogene samples in the IMR and CMB (Fig. 17) appears, at first, to suggest that sediments were derived from the same source as those in the CMB – that is, from the WPA (e.g. Allen *et al.* 2008; Naing *et al.* 2014; Wang *et al.* 2014; Licht *et al.* 2019; Najman *et al.* 2020; P. Zhang *et al.* 2019). However, the Kalembo–Nagaland suture zone, which we correlate with the Himalayan IYTSZ, containing Jurassic and Cretaceous ophiolites, deep ocean sediments and volcanics, points to the IMR being separated from the CMB. This suture finally closed at *c.* 50 Ma (Green *et al.* 2008) or even 60 Ma (Kapp and DeCelles 2019), suggesting that, prior to closure, the IMR were separated from the CMB by the closing Neotethys Ocean. However, there is significant provenance and stratigraphic evidence to suggest that the closure was complex and there is conflicting evidence for regarding how closure occurred.

The provenance of sediments in the CMB has largely been assessed through petrography, zircon, titanite and apatite U–Pb

dating and geochemistry, rutile geochemistry and Sr–Nd bulk analyses to identify arc-derived sediment input from input derived from the continental crust (Licht *et al.* 2013, 2016, 2019; Wang *et al.* 2014; Cai *et al.* 2020; Arboit *et al.* 2021; X. Zhang *et al.* 2021; Najman *et al.* 2022). Commonly in these studies, the arc component is thought to be derived from the WPA, whereas the crustal component is considered to be derived from the Himalaya or the Mogok Metamorphic Belt, along with the Kanpetlet Schists and Pang Chaung Formation. Although there is widespread agreement in these studies that the Paleocene–middle Eocene sediments contain a significant component of material derived from the WPA, there is more divergence of interpretation for the provenance of the post-middle Eocene section, which shows more crustally derived sediment. In particular, it is disputed whether the Mogok Metamorphic Belt rocks were a key early source of sediment. A late Mid-Eocene to Late Eocene arrival of sediments sourced from the Mogok Metamorphic Belt in the CMB has been proposed by Licht *et al.* (2019), X. Zhang *et al.* (2021) and Arboit *et al.* (2021), whereas Westerweel *et al.* (2020), Morley *et al.* (2021) and Najman *et al.* (2022) considered that the early metamorphic component was

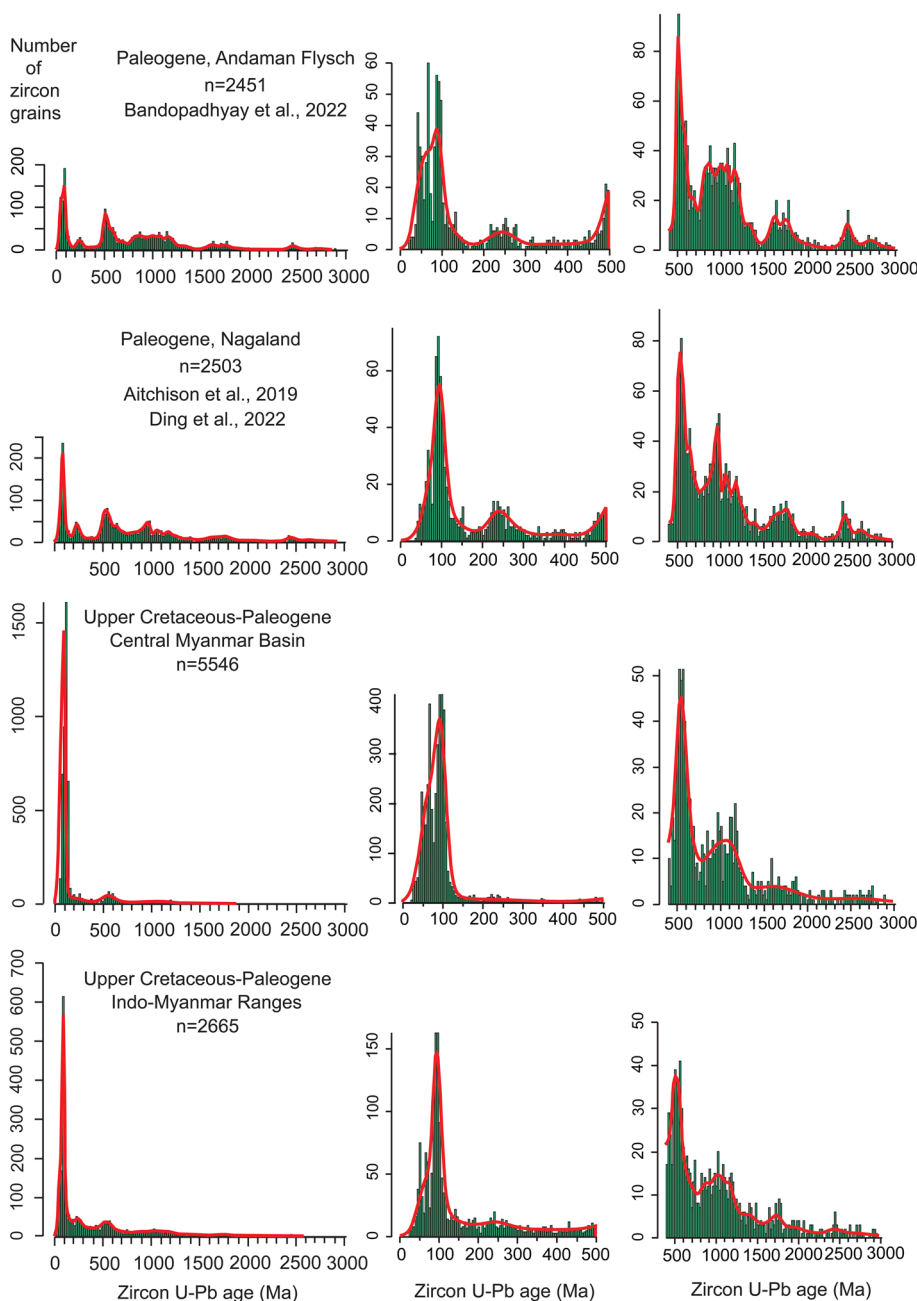


Fig. 17. Comparison of detrital zircon U–Pb data from the Indo-Myanmar Ranges (Naing *et al.* 2014; Allen *et al.* 2008; Najman *et al.* 2020; this study), with those from Central Myanmar Basin (Wang *et al.* 2014; Cai *et al.* 2020; Licht *et al.* 2019; P. Zhang *et al.* 2019; X. Zhang *et al.* 2021; Arboit *et al.* 2021; Najman *et al.* 2022; this study), Nagaland (Aitchison *et al.* 2019; Ding *et al.* 2022) and the Andaman Flysch (Bandopadhyay *et al.* 2022). All ages are displayed in 20 Ma bins (0–3000 Ma, 400–3000 Ma) and 5 Ma bins (0–500 Ma). Ordinate axis indicates the number of detrital zircon ages in each bin on the abscissa.

derived from within the WMT (for example, the Naga Metamorphic Complex). One major issue for the Mogok Metamorphic Belt rocks being an Eocene–Oligocene sediment source is that, at this time, these rocks were experiencing amphibolite to granulite grade regional metamorphism (e.g. Searle *et al.* 2007, 2020; Lamont *et al.* 2021). Exhumation and retrograde metamorphism only occurred after *c.* 30 Ma (Searle *et al.* 2017) and, in places, after 20 Ma (Lamont *et al.* 2021). Even during the Early Miocene, micas were forming in the basement rocks of the Shan Scarp during deformation at temperatures between 250 and 300°C (Bertrand *et al.* 2001). By contrast, the derivation of zircons from the Naga Metamorphics to the south of Mt Saramati (i.e. within the WMT) seems more plausible than the Mogok Metamorphic Belt rocks because these schists and gneisses containing Early Ordovician age zircons were uplifted and eroded by the Eocene (Aitchison *et al.* 2019). The Katha Metamorphic rocks, to the north of the Mogok Metamorphic Belt, have been suggested as a possible additional source of sediment to the CMB, but this seems unlikely given that they were exhumed relatively late, between 40 and 15 Ma (Min *et al.* 2022).

Our detailed comparison of the IMR and CMB data shows that the petrographic, zircon age spectra and Hf isotope data exhibit several subtle differences between the Upper Cretaceous samples from the two regions. Samples from the Upper Cretaceous Kabaw Formation in the CMB fall in the undissected arc field and indicate the WPA was the proximal magmatic arc source (Wang *et al.* 2014; Cai *et al.* 2020; this study). Upper Cretaceous Falam Formation sandstones from the IMR contain less abundant volcanic lithics than those from the CMB (Fig. 9e, f) and indicate a recycled orogenic provenance falling in the transitional and undissected arc fields (Fig. 8). However, the more distal position of the Falam Formation can explain the difference as a loss of the more unstable volcanic lithic component during transport. When considering details of the zircon age spectra, the Kabaw and Falam formations display prominent peaks at 110–90 Ma (Fig. 18a, b). The Cretaceous CMB zircons have entirely positive ϵ_{Hf} values; Cretaceous zircons from the IMR are also characterized by positive ϵ_{Hf} values, indicating a juvenile mantle source. However, a few grains with negative ϵ_{Hf} values, indicative of the re-melting of older crust, are also present in the IMR samples (Fig. 18e, f). The detrital zircon characteristics of the Upper Cretaceous Falam Formation are therefore slightly different from those of the Kabaw Formation. The new provenance data from the Falam Formation indicate that detritus from contemporaneous volcanic rocks was mixed with sediment recycled from older siliciclastic units. The maximum depositional age (84 ± 1 Ma) determined from the zircon geochronology is close to the actual depositional age of the sediments and indicates that contemporaneous magmatism had an important role in the morphological evolution of the source region. U–Pb zircon and whole-rock Ar–Ar ages for the Mawgyi volcanics from the Wuntho Ranges include ages between 110–90 Ma and 46–32 Ma (Li *et al.* 2019; Westerweel *et al.* 2019; Licht *et al.* 2020; Fig. 10), but Upper Cretaceous zircons younger than 90–85 Ma are unknown (Licht *et al.* 2020).

Mitchell (1992, 1993) interpreted the Mawgyi Nappe as an intra-oceanic arc that was emplaced onto the western margin of SE Asia along with the Woyla Arc of Sumatra during the mid-Cretaceous. In this model, the CMB/Myanmar Terrane (the ‘Burma Terrane’ of Mitchell 1992, 1993) did not exist as a separate entity during the Cretaceous. However, palaeomagnetic data indicate that the Myanmar Terrane was a separate entity during the Cretaceous and was too far south in the Cretaceous to be part of the SE Asian margin (Westerweel *et al.* 2019). This model is incompatible with the Mawgyi Nappe model. The peak of WPA volcanism (including the Mawgyi volcanics) at *c.* 100 Ma indicates active subduction in the vicinity of the IMR/CMB. The Mawgyi volcanics are therefore most

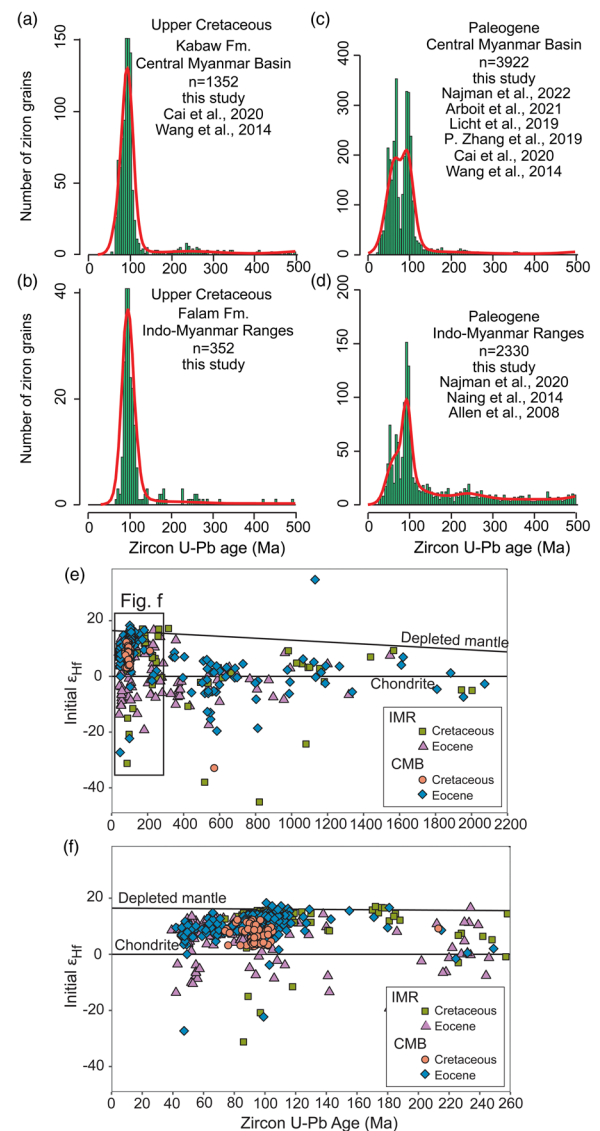


Fig. 18. Comparison of detrital zircon U–Pb ages and Hf isotopic data. (a, b) Upper Cretaceous Falam Formation, Indo-Myanmar Ranges and Kabaw Formation, Central Myanmar Basin. (c, d) Paleogene units, Indo-Myanmar Ranges and Central Myanmar Basin. (e, f) Late Cretaceous–Middle Eocene Hf isotopic data from the Indo-Myanmar Ranges (Naing *et al.* 2014; this study) and the Central Myanmar Basin (Wang *et al.* 2014; P. Zhang *et al.* 2019). Ordinate axis indicates the number of detrital zircon ages in each bin on the abscissa. Bin size is 20 Ma.

likely part of the WPA and can probably be correlated with the intra-oceanic mid-Cretaceous Woyla Arc. The onset of the Woyla Arc collision with Sumatra at 113 Ma (Advokaat *et al.* 2018) occurred close to the time at which the Aptian–Cenomanian Limestone unconformity developed and the formation of the metamorphic sole in the Inner Belt of the IMR (J.E. Zhang *et al.* 2017), indicating a possible link between the unconformity, ophiolite emplacement and the Woyla Arc collision. In their interpretation, Morley *et al.* (2020) proposed that the Mt Victoria Terrane collided with the western side of the WMT and that the ophiolites are unconformably overlain by Aptian–Cenomanian limestones (Mitchell 1993). Deposition of the Falam and Kabaw formations initiated at *c.* 84 Ma and both unconformably overlie the Mesozoic IMR units (Kanpetlet Schists, Pane Chaung Formation). This unconformable relationship indicates that the Inner Belt of the IMR and the CMB were part of the same plate by the Late Cretaceous (Morley *et al.* 2021). The Falam Formation was therefore derived mainly from the Wuntho Ranges,

with a subordinate input from a more crustal source, potentially the Ordovician Nagaland metamorphic rocks (Aitchison *et al.* 2019).

Allen *et al.* (2008); Naing *et al.* (2014) and Najman *et al.* (2020) suggested that Paleogene sandstones of the IMR were derived predominantly from the WPA to the east, rather than scraped off the Himalayan-derived Bengal Fan material as proposed earlier (Curry 2005). This conclusion is based on the more arc-like provenance signatures, as evidenced by petrography and the proportions of arc-derived Mesozoic–Paleogene zircons. Comparison of the IMR data with that of the CMB (Naing *et al.* 2014; Wang *et al.* 2014; Licht *et al.* 2019; P. Zhang *et al.* 2019; Cai *et al.* 2020; Najman *et al.* 2020, 2022; Arboit *et al.* 2021; this study) shows that the age spectra for the IMR and CMB were similar in the Paleogene. However, a detailed comparison indicates differences in the zircon age spectra. Detrital zircons from Paleogene sandstones in the IMR show a notable age peak at 90 Ma, whereas the CMB has a major age peak at 90 Ma and a lesser peak at c. 60 Ma (Fig. 18c, d). Zircon U–Pb age clusters for the IMR match well with the WPA magmatism (Mitchell *et al.* 2012; Gardiner *et al.* 2016, 2018; P. Zhang *et al.* 2017). New and published (Naing *et al.* 2014) Hf isotope data from Cretaceous–Eocene zircons from the IMR show that the ϵ_{Hf} values are predominantly positive, with only a few grains with negative ϵ_{Hf} values (Fig. 18e, f). This IMR signature contrasts with data from the CMB (Wang *et al.* 2014; P. Zhang *et al.* 2019). On the QFL and LmLvLs plots, Paleogene sandstones from the IMR lie within the magmatic arc field (Fig. 8b, c). New data and previously published work (Allen *et al.* 2008; Naing *et al.* 2014; Najman *et al.* 2020) clearly show additional older crustal material identified petrographically as low-grade metamorphic and siltstone lithic fragments, by negative ϵ_{Hf} values, and by the presence of Paleozoic and older zircons and older fission track ages. These data all indicate that the Paleogene IMR contains a significant component of arc-derived material from the WPA, with a subordinate component of crustal-derived material from the Kanpetlet Schists and Naga metamorphic basement.

If the palaeomagnetic model of Westerweel *et al.* (2019) is viable, then the Paleozoic and older ‘Myanmar basement’ that provided the old zircons could not have been the Shan Plateau region because the separation from the IMR involved several hundred kilometres of oceanic crust between the two regions.

The peak of c. 100 Ma age for zircons of arc-affinity strongly indicates the WPA as a source for the Falam Formation. The absence of older zircons is also significant in eliminating the possibility of any Indian source. These observations are important

because it is commonly considered that the deep-water, shale-prone Falam and Chunsang formations are lateral equivalents of the Disang Formation in India. However, as discussed here, they are predominantly sourced from the WMT (i.e. they occupied an upper plate position), whereas the Disang Formation appears to be predominantly sourced from India (Aitchison *et al.* 2019; Ding *et al.* 2022) (Fig. 17) (i.e. a lower plate position). These conclusions are based on relatively few studies of a limited number of samples from geographically restricted areas and a lateral transition between these India- and WMT-sourced deep-water deposits involving mixed sources probably exists, perhaps in the Manipur area.

The difference in source area for the Falam and Disang formations is crucial in respect of the origins of the Pane Chaung Formation. The Indian provenance of the Disang Formation makes it possible to argue that the Pane Chaung Formation is part of the Indian margin that collided with the WMT in the Cenozoic. The presence of the WMT-derived Falam Formation overlying, and to the west of, the Pane Chaung Formation implies that this Triassic formation was present on the WMT margin prior to the Late Cretaceous and therefore unlikely to have been part of the leading edge of India.

Relationship with the IYTSZ

It is debated whether two ophiolite belts (the Kalemmyo Ophiolite/Western Ophiolite Belt and the Myitkyina Ophiolite/Eastern Ophiolite Belt) within Myanmar belong to a single suture; furthermore, their relationship with the IYTSZ in the Tibetan Plateau is not clear (Mitchell 1993; Yang *et al.* 2012; Morley *et al.* 2021). Recent radiometric dating and geochemical studies on ophiolites in Myanmar and Tibet are summarized in Table 2.

The Nagaland–Kalemmyo zone of ophiolites of the IMR (the Western Ophiolite Belt) contains fragments of Cretaceous oceanic lithosphere, Mesozoic radiolarian cherts, alkaline volcanic rocks and mélanges very similar to the IYTSZ in Tibet. The mineralogical and geochemical characteristics of the Nagaland–Kalemmyo zone of ophiolites indicate that both mid-ocean ridge and supra-subduction zone affinity types are present (Ghose *et al.* 2014; Liu *et al.* 2016b; J. Zhang *et al.* 2018), similar to ophiolites along the IYTSZ (Table 2). Moreover, the discovery of well-preserved Middle Jurassic–Late Jurassic radiolarian assemblages from the Kalemmyo Ophiolite (J. Zhang *et al.* 2018; this study) and Naga Ophiolite (Baxter *et al.* 2011; Aitchison *et al.* 2019), and Early Cretaceous assemblages from the Manipur Ophiolite (Aitchison *et al.* 2019), provides age constraints on deep-marine sedimentation that are consistent with those reported

Table 2. Summary of published data on ophiolite formation and emplacement in the Indo-Myanmar Ranges and Tibet

Locality of suture zone	Ophiolite formation in a nascent arc (Ma)	Ophiolite generation in the subduction zone (Ma)	Environment of formation	Presence of HP–LT metamorphism	Dating of ophiolite emplacement	References
Tibet						
Indus–Yarlung Tsangpo suture zone	177–150	130–88	MOR and SSZ	Yes	Late Cretaceous	Hébert <i>et al.</i> (2012)
Kalemmyo		127	MOR	No	Pre-Mid-Cretaceous	Liu <i>et al.</i> (2016b), J.E. Zhang <i>et al.</i> (2017), J.E. Zhang <i>et al.</i> (2017), J. Zhang <i>et al.</i> (2018)
Indo-Myanmar Ranges						
Naga–Manipur		118–116	MOR and SSZ	Yes	Late Eocene–Early Oligocene	Baxter <i>et al.</i> (2011), Ningthoujam <i>et al.</i> (2012), Ghose <i>et al.</i> (2014), Singh <i>et al.</i> (2017), Aitchison <i>et al.</i> (2019)
Andaman Islands		95 ± 2	SSZ	No	Paleogene	Pedersen <i>et al.</i> (2010), Ghosh <i>et al.</i> (2009), Pal (2011)

HP, high-pressure; HT, high-temperature; MOR, mid-ocean ridge; SSZ, super-subduction zone.

from ophiolites in Tibet (Fig. 14a, b) and reinforces the hypothesis that these ophiolites were once part of the same Neotethyan ocean floor.

Comparison of the timing of events in the IYTSZ (e.g. reviews in Hébert *et al.* 2012; Kapp and DeCelles 2019) with those in the IMR is instructive. Kapp and DeCelles (2019) proposed the following key events associated with the IYTSZ. (1) Jurassic ophiolites formed in a forearc or an intra-oceanic arc setting (e.g. McDermid *et al.* 2002; Aitchison *et al.* 2007). (2) Lower Cretaceous ophiolites formed in a proximal position to the Lhasa Terrane in a forearc extensional or intra-oceanic arc setting (e.g. Hébert *et al.* 2012), including local developments within Jurassic oceanic crust, possibly related to the re-initiation of subduction or due to slab rollback. (3) A 120–105 Ma high-intensity magmatic belt developed, coeval with widespread marine limestone deposition over the Lhasa Terrane. This magmatic event is not seen in the Gangdese Arc. (4) A 90–80 Ma tectonothermal event involving metamorphism and magmatism was followed by a quiescent period of uncertain origin in the Gangdese Arc between 78 and 72 Ma, but possibly related to slab rollback or the subduction of a slab window. (5) Intra-arc or retro-arc shortening of the Gangdese magmatic arc, accompanied by metamorphism, and a high-intensity magmatic event from 70 to 45 Ma, together with shortening within the northern Lhasa and Qiangtang terranes. Initially, this event was related to Cordillera-style deformation, which, at *c.* 60 Ma, probably evolved to India–Asia collision. The timing of these elements in the IYTSZ (particularly events 1, 2 and 3) is very much in line with the IMR (Liu *et al.* 2016b; Aitchison *et al.* 2019; Morley *et al.* 2020): (1) with the Jurassic events in the Inner Belt (Jurassic-aged chert); (2) the ages of the Kalemio and Nagaland oceanic lithosphere fragments formed at *c.* 130–115 Ma; and (3) the occurrence of high-pressure metamorphic rocks (i.e. blueschist, glaucophane schist, jadeitite and eclogite) in Nagaland and the Jade Belt.

In a review of the Nagaland Ophiolite data, Bhowmik *et al.* (2022) concluded there is evidence for a collage of a Late Triassic

to Mid-Jurassic (*c.* 205–172 Ma) intra-oceanic (Neotethys) subduction system, as well as a later subduction system that ended with India–Myanmar collision during the Eocene. In Nagaland, the peak high-pressure–low-temperature metamorphism is estimated to have occurred at *c.* 95 Ma, whereas retrograde metamorphism during shear-related exhumation is dated at *c.* 90 Ma (Maibam *et al.* 2022). The divergences between intense magmatic activity in the WMT (42–36 and 108–90 Ma) and the Gangdese Arc (190–160, 60–40 and 20–10 Ma) and the North Lhasa Plutonic Belt (120–105 and 25–15 Ma) are significant (Licht *et al.* 2020) for the later history of the region. Nevertheless, similarities in the timing of events between the Kalemio Ophiolite and the Neotethyan ophiolites suggest that the Western Ophiolite Belt is the southern continuation of the IYTSZ on the Tibetan Plateau (Liu *et al.* 2016a).

Tectonic models for the IMR and WMT

The position of the suture between India and Asia in Myanmar remains uncertain and different tectonic scenarios have resulted in three proposals for the location of sutures (Fig. 19): (1) concealed beneath overthrust Cretaceous–Cenozoic deep-water sediments in the outer IMR (Fig. 19a–c, location 1); (2) along the Western and Eastern Ophiolite belts (Fig. 19a–c, location 2); and (3) between the ‘West Myanmar Block’ and Sundaland (Fig. 19b location 3).

Location 1 is related to the interpretation that there is active subduction of oceanic crust and/or the under-thrusting of the leading edge of India below the IMR based mostly on geophysical data (seismicity, mantle topography and gravity) (Steckler *et al.* 2008; Yang *et al.* 2022). Location 1 can simply be viewed as a continuation of the suture in location 2 following westwards slab rollback and the addition of sediment to the distal part of the accretionary prism (Fig. 19b, c). Alternatively, Socquet *et al.* (2002) proposed a scenario where locations 1 and 2 were two distinctly

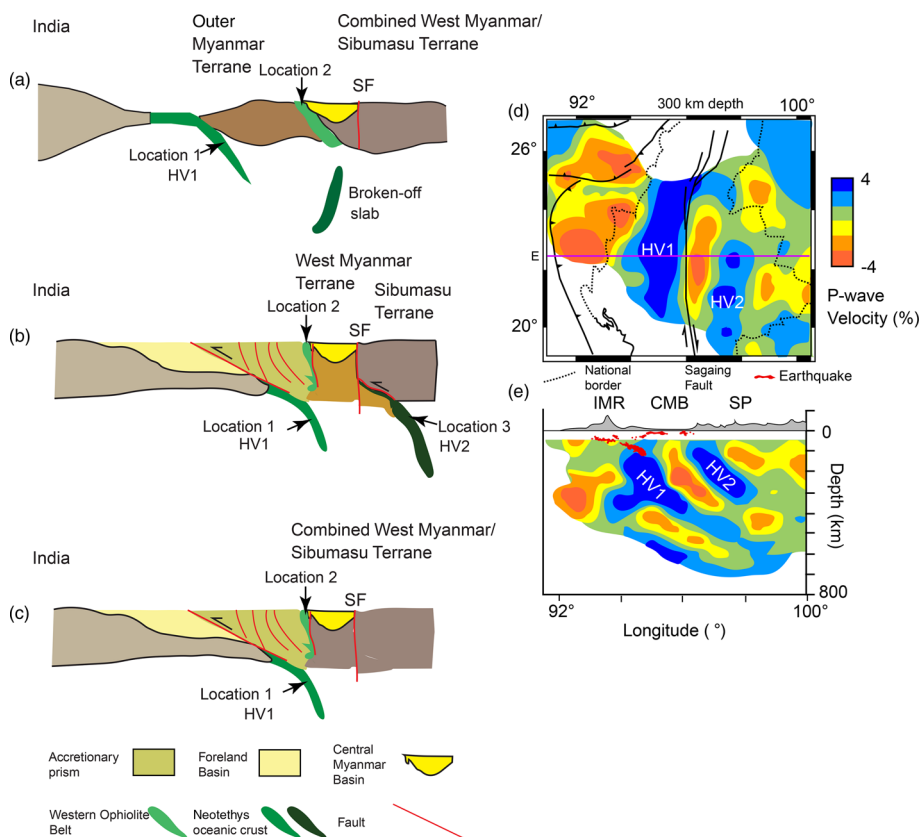


Fig. 19. Schematic cartoon cross-sections across the Indo-Myanmar Ranges from India to the Shan Plateau illustrating the potential location of suture zones according to different tectonic models. (a) West Myanmar Terrane model of Socquet *et al.* (2002). (b) Independent West Myanmar Terrane model (e.g. Westerweel *et al.* 2019; Morley *et al.* 2020). (c) West Myanmar Terrane as part of SE Asia since the Indosinian Orogeny (e.g. Sevastjanova *et al.* 2016; Morley 2018). Results of mantle tomography study centred on Myanmar (redrawn from Yang *et al.* 2022): (d) time slice at 300 km and (e) depth section, see part (d) for location. CMB, Central Myanmar Basin; HV1, high-velocity zone 1; HV2, high-velocity zone 2 (interpreted as subducted slabs); IMR, Indo-Myanmar Ranges; SF, Sagaing Fault; SP, Shan Plateau.

separate sites of Cenozoic suturing. In this scenario, Late Cretaceous–Paleocene obduction occurred between an eastern continental block consisting of the Shan Plateau sequence of Sundaland and the CMB area, and a microcontinent they referred to as the ‘Bloc Ouest Birman’, which lay west of an ophiolitic suture (location 2, Fig. 19a). In this scenario, their ‘Bloc Ouest Birman’ is a different entity from the WMT in this study, which is typically envisioned as underlying the CMB and lying predominantly east of the ophiolites (Fig. 19b; see discussion in Morley *et al.* 2021).

Location 2 is related to the presence of numerous ophiolitic fragments along the core region of the IMR (the Western Ophiolite Belt). The characteristics of these fragments are similar to those described for the IYTSZ. It can be further argued that the Pane Chaung Formation is of Indian affinity and, consequently, immediately west of the suture are units related to India, whereas east of the suture are units related to West Myanmar (which, in turn, may have been attached to Sundaland). However, the situation is not that simple because the Falam Formation is predominantly sourced from the WMT. Nevertheless, location 2 has a number of basic attributes that make it an obvious candidate for the suture zone between India and West Myanmar.

Location 3 (Fig. 19b) roughly separates Sundaland to the east from the West Myanmar plate to the west, yet there is no clear geological evidence for a suture zone. Virtually no outcropping ophiolitic rocks or Neotethyan oceanic domain rocks have been described along the trend. It is difficult to define where the West Myanmar plate ends and Sundaland begins. The only well-defined boundary is the transform margin along the Sagaing Fault, which is predominantly a Neogene age feature. There are ultrabasic rocks along the Sagaing Fault, but it is also possible to interpret the paired magmatic belts of Central Myanmar and the western Shan Plateau region in terms of an Andean subduction model (e.g. Mitchell 1993; Gardiner *et al.* 2015), which implies close proximity of the two terranes throughout the Cenozoic. In spite of these issues, palaeomagnetic data provide a key piece of evidence that forces location 3 to potentially be considered as a major suture. Samples from Late Cretaceous and Paleogene igneous and sedimentary localities provide consistent data that show the WMT migrated from south of the equator during the Late Cretaceous to a location about 5° N in the Late Eocene (Westerweel *et al.* 2019, 2020), implying significant loss by subduction of Tethyan oceanic crust between West Myanmar and Sundaland during the Cenozoic (see discussion in Morley *et al.* 2021). There is a suggestion that a slab can be identified below the Shan Plateau from mantle tomography, which supports the existence of this suture (Yang *et al.* 2022) (Fig. 19d, e).

Of the three locations, location 2 has many elements common to other suture zones and is thus, arguably, a good candidate to mark the suture between India and West Myanmar. To assess this idea further, consideration of the timing of events at location 2 is key. The western margin of the CMB shows a stratigraphic sequence that consists of mid-Cretaceous *Orbitolina* limestone (the Paung Chaung Formation) overlain by the Upper Cretaceous, shale-prone Kabaw Formation and the upper Paleocene Paunggyi Conglomerate. These sequences extend under the CMB (i.e. they are part of the WMT) and also overlie the eastern margin of the IMR. Only the Manaung Chaung area in the Southern Chin Hills is cited as a locality where pillow lavas associated with the core region of the IMR are seen unconformably underlying the Paung Chaung Formation (United Nations 1979; Mitchell *et al.* 2010; Mitchell 2017). However, given the inconclusive evidence for a clear unconformable contact, one possibility for location 2 is that the Paung Chaung Formation does not unconformably overlie the ophiolites, but is in faulted contact. Rangin *et al.* (2013) cited the occurrence of ophiolite clasts in the Kabaw Formation as evidence for Maastrichtian-age obduction. However, the 115 Ma age for the metamorphic sole of the Kalemmyo Ophiolite (Liu *et al.* 2016b) is

more consistent with the Paung Chaung Formation marking the time shortly after obduction than the Kabaw Formation. The mapped unconformable contacts between the Pane Chaung Formation and both the Paung Chaung Formation and the Kabaw Formation are widespread (United Nations 1979; see review in Morley *et al.* 2020). Although the Paung Chaung Formation unconformity can be seen on geological maps, but has no clear contact in outcrop (United Nations 1979), the Pane Chaung and Kabaw Formation unconformity is observable and documented from outcrop (Socquet *et al.* 2002; Rangin *et al.* 2013; P. Zhang *et al.* 2017; Cai *et al.* 2020). Triassic detrital zircon peaks, and the predominantly schist and quartz composition of clasts in conglomerates of the lower Kabaw Formation, suggest that the sediment source was the Pane Chaung Formation and Kanpetlet Schists (Cai *et al.* 2020). This unconformable relationship is crucial because it indicates that, whatever tectonic entity the Pane Chaung Formation was deposited on (whether the leading margin of India, the Mt Victoria microplate or the WMT; see discussion in Morley *et al.* 2020), it was overlain by sequences related to the CMB during the Late Cretaceous.

Although it is within the same belt as the Chin Hills and Kalemmyo ophiolites, the age of the Naga Ophiolite is different and also needs to be considered in an assessment of location 2 as a potential suture. The Naga Ophiolite is interpreted to have formed in a supra-subduction zone setting at *c.* 116 Ma based on the U–Pb zircon age of plagiogranites and gabbros (Singh *et al.* 2017; Aitchison *et al.* 2019) – that is, very close to the age of the metamorphic sole of the Kalemmyo Ophiolite. The Naga Ophiolite assemblage has subsequently been thrust over a *mélange* that contains Paleogene–Eocene radiolarians (Aitchison *et al.* 2019). This ophiolite emplacement is interpreted to be related to the collision of Greater India within an intra-oceanic island arc around the Paleocene–Eocene boundary (*c.* 55 Ma) (Aitchison *et al.* 2019). Although it is feasible for the emplacement of accretionary-type ophiolites to occur at any time during the life of an accretionary prism, we also have dating of a metamorphic sole (119 ± 3 to 115 ± 1 Ma; Liu *et al.* 2016b; J.E. Zhang *et al.* 2017) indicating Early Cretaceous emplacement and stratigraphic evidence for some of the ophiolites in Myanmar to have been emplaced during the Late Cretaceous (e.g. Mitchell 1993; Mitchell *et al.* 2010; Rangin *et al.* 2013). Consequently, does the thrusting of the Naga Ophiolite onto Paleogene sedimentary units represent a Paleogene episode of ophiolite emplacement, or thrusting and reworking of an older ophiolite emplaced during the Cretaceous as a consequence of the onset of the collision of India with West Myanmar? This phase of ophiolite thrusting and exhumation is capped by the Late Eocene–Early Oligocene Phokphur Formation, which was deposited in shallow marine to fluvial environments and contains abundant ophiolite fragments and detrital zircons from a Permo-Triassic source, possibly the Pane Chaung Formation (Aitchison *et al.* 2019) (Fig. 15).

Based on this discussion of the timing of events on both the western CMB margin and the Naga Ophiolite, it would appear that location 2 marks a succession of ophiolite deformation events beginning at 115 Ma with the emplacement of the Kalemmyo Ophiolite (Liu *et al.* 2016b), followed by thrusting, uplift and erosion prior to deposition of the Paung Chaung Formation (Mitchell 1993). Peak metamorphism and exhumation of blueschists occurred between 95 and 90 Ma (Maibam *et al.* 2022), with uplift and erosion during the Maastrichtian deposition of the Kabaw Formation (Socquet *et al.* 2002). Thrusting of the Naga Ophiolite over Paleogene *mélange* took place at *c.* 55 Ma (Aitchison *et al.* 2019). These disparate histories of the two ophiolites are consistent with a complex history of accretion on the western margin of the WMT.

The change from deep-water sedimentation to molasse sedimentation in the IMR began, in places, in the Late Eocene (e.g. Aitchison *et al.* 2019; see review in Morley *et al.* 2020), which strongly indicates that India and West Myanmar had collided by this

time. Low-temperature thermochronology from three transects, which shows the timing of the onset of exhumation, varies between *c.* 24 Ma (the Kalembo–Kennedy Peak transect) and *c.* 50–49 Ma (Mindat section) (Najman *et al.* 2022). These results are not straightforward to interpret in terms of the onset of deformation because cooling will largely be related to erosion, which requires subaerial exposure, or extension, which would post-date compressional or transpressional deformation. Deformation will initially cause burial, not the exhumation of a unit in the footwall of a major thrust. In a submarine wedge, even the hanging wall of a major thrust might not be subject to significant erosion (action by currents and gravitational instability can cause some degradation). Consequently, what the cooling ages may indicate is a transition from submarine to subaerial exposure of parts of the wedge. The *c.* 50 Ma age for the exhumation of the inner area of the IMR suggests: (1) the timing of the onset of India–West Myanmar collision was Early Eocene (Searle and Morley 2011; Najman *et al.* 2022); (2) the inner area of the IMR was close to sea-level even before collision; and (3) the outer IMR remained as a submarine wedge for much longer (into the Miocene).

There are other possible causes for exhumation besides collision with the leading edge of Greater India, such as the subduction of an unusually thick or buoyant piece of crust (e.g. a seamount or mid-ocean ridge), or an increase in sediment supply to the accretionary prism, such as the Bengal Fan (Najman *et al.* 2022). Other strands of evidence that support India–West Myanmar collision are as follows. The rapid northwards motion of West Myanmar from the Eocene to the Miocene based on palaeomagnetic data is best explained by coupling with India at *c.* 60 Ma (Westerweel *et al.* 2019, 2020). The Paleocene–early Miocene timing of metamorphism along the Mogoke Metamorphic Belt (Searle *et al.* 2020; Lamont *et al.* 2021) and the 40–30 Ma rapid exhumation of the Katha Ranges, which lie between the Jade Belt and the Eastern Ophiolite Belt, also support Eocene age continent–continent collision (Min *et al.* 2022). Consequently, it is considered that location 2 fits well with Eocene collision between India and the WMT.

From this review, location 2 marks a long-lived zone where a major segment of the Neotethys Ocean was closed during the Mesozoic and Paleogene. However, it does not appear to have accommodated convergence and the loss of significant oceanic crust

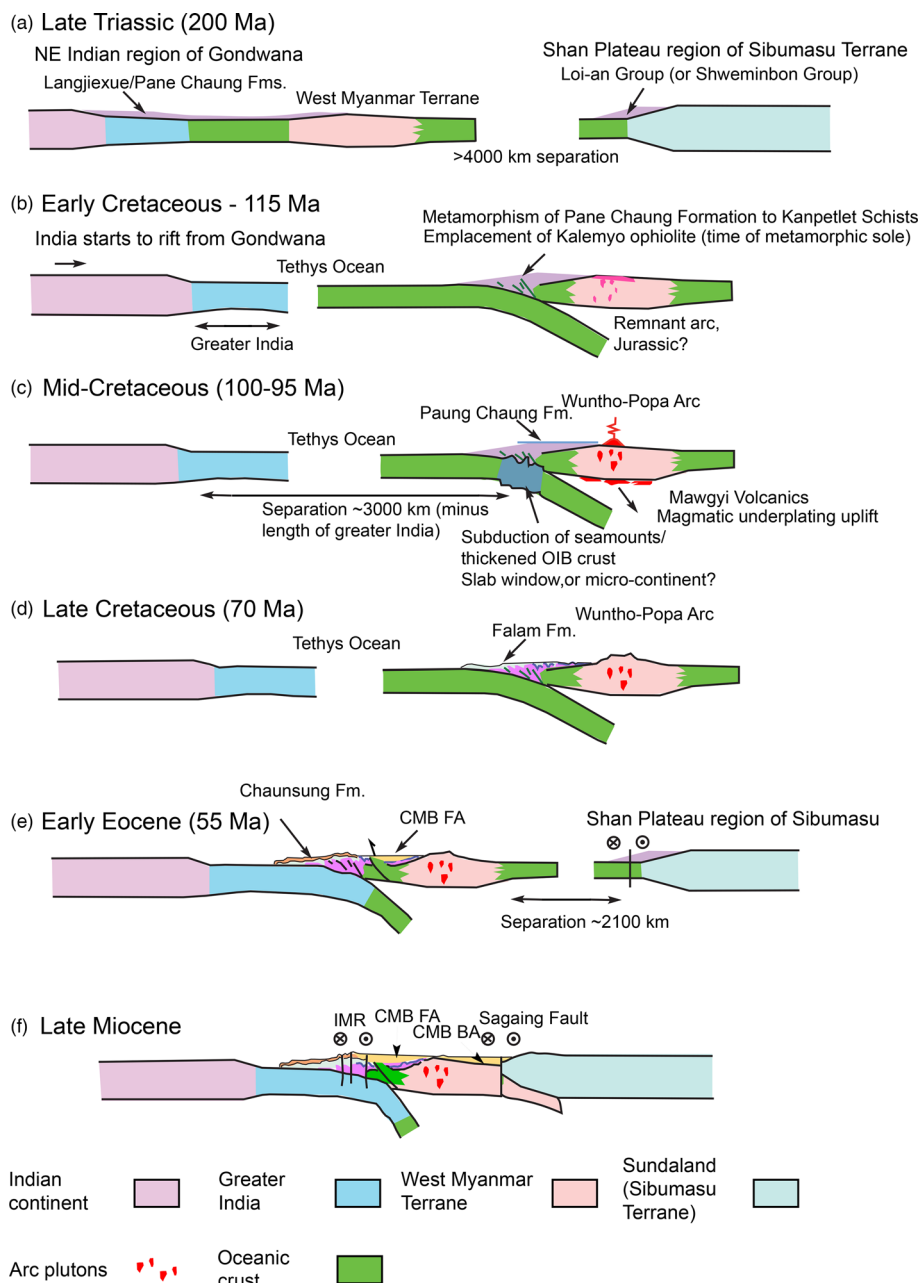


Fig. 20. Tectonic model explaining the development of the Indo-Myanmar Ranges through time. CMB-FA, Central Myanmar Basin-Forearc; CMB-BA, Central Myanmar Basin-Back-arc; OIB, ocean island basalt. Source: modified from Morley *et al.* (2020).

from the Oligocene to Recent. This leaves convergence to be accommodated at location 3. As noted earlier, there is virtually no geological evidence for a suture, it is very difficult to locate what constitutes the eastern boundary of the WMT, and there are multiple possible scenarios for how the WMT interacted with the Andaman Sea region, as discussed in [Morley *et al.* \(2021\)](#) and [Bandopadhyay *et al.* \(2022\)](#). These various scenarios have such poor correlation with known geological events and tectonic elements in the Andaman Sea that they were not features of tectonic models for the area until the palaeomagnetic data forced such considerations ([Morley *et al.* 2021](#)). The solution of [Bandopadhyay *et al.* \(2022\)](#) helps to resolve the issue of the absence of a suture in Myanmar by having a Paleocene–early Eocene collision of the WMT with the Andaman Islands. However, there remains little direct geological evidence for such a collision and, for the scenario to be feasible, the palaeomagnetic data of [Westerweel *et al.* \(2019\)](#) was re-interpreted so that the positions of the WMT, most critically during the Oligocene, lie further north than the original interpretation. Although the provenance data for the East Andaman Flysch is compatible the WMT being one of the sources ([Bandopadhyay *et al.* 2022](#)) ([Fig. 17](#)), it does not resolve whether this source lay to the west ([Bandopadhyay *et al.* 2022](#)) or to the north ([Morley *et al.* 2021](#)) of the Andaman Islands.

A possible tectonic scenario is shown in [Figure 20](#). Because the Kabaw Formation unconformably overlies the Pane Chaung Formation on the western margin of the IMR, and the Falam Formation is sourced from the WMT, it is necessary for the Pane Chaung Formation to be part of the WMT prior to the Late Cretaceous. Hence the WMT is shown as being close to India, perhaps in a rifted setting, and the Pane Chaung Formation was deposited across the rift on both the Indian and WMT margin ([Fig. 20a](#)). Subsequently, subduction below West Myanmar incorporated the Pane Chaung Formation in an accretionary prism, where slivers of ophiolite were emplaced, and Jurassic oceanic sediments were incorporated into accretionary mélangé (location 2, [Figs 19, 20b](#)). During the mid-Cretaceous, the WMT underwent uplift, possibly as a consequence of magmatic underplating (collision with the Mt Victoria Terrane, subduction of a slab window or a seamount are other possibilities; [Fig. 20c](#)) and the Paung Chaung Formation carbonates were deposited over part of the accretionary prism. The accretionary prism built out oceanwards as the Falam and Chunsang formations, predominantly sourced from the WMT ([Allen *et al.* 2008](#); [Naing *et al.* 2014](#); [Najman *et al.* 2020](#); this study) built out over oceanic crust ([Fig. 20d](#)). The Paleogene part of the Disang Formation in India may be equivalent to the Chunsang Formation and shows evidence for both a far-travelled sediment source from India and a closer sediment source from the core region of the IMR to the east ([Imchen *et al.* 2014](#)). During the Early Eocene, the highly extended leading edge of the Indian continent began to collide with the WMT ([Fig. 20e](#)). The coupled India–WMT region also began its highly oblique convergence with the Shan Plateau region of the Sibumasu Terrane on the western Sundaland margin ([Fig. 19b](#), location 3). Evolution into a transform margin marked by the Sagaing Fault began during the late Cenozoic ([Fig. 20f](#)).

Conclusions

Determining the age of deep-water sandstone–shale sequences in the Inner IMR remains problematic. Detrital zircon age spectra for sandstones provide a useful check of lithostratigraphic and biostratigraphic correlations. The mapped extent of Paleogene strata has been modified by the recognition of the Triassic Pane Chaung Formation in the southern IMR (the Gwa Road section area) and the discovery of Paleogene-age detrital zircons within rocks previously thought to be of Late Cretaceous age (the Padaung–Taungup road section). Detrital zircons confirm an Eocene age for

the Kennedy Sandstone with a maximum depositional age of 43 ± 2 Ma. Radiolarian cherts from the Yazagyo Dam area indicate Late Jurassic (Unitary Association Zones 9–11) biogenic deposition on oceanic crust and represent a rare record of sedimentation between that of the thicker clastic deep-water deposits of the Pane Chaung Formation (Upper Triassic–Lower Jurassic?) and the Upper Cretaceous Falam Formation.

Provenance analysis of the Pane Chaung Formation supports correlation with the Langjiexue Group in the northern Tethys Himalaya, considerably reducing the number of viable tectonic models for the origin of the IMR/WMT. The Pane Chaung Formation was deposited on the northern margin of India or on a continental block adjacent to India and rifting of that continental fragment from Gondwana can only have occurred during the Jurassic or Early Cretaceous. Whether the Pane Chaung Formation was part of West Myanmar from inception, or a later accreted continental fragment (Mt Victoria Land), remains uncertain. The Western Ophiolite Belt represents the southern extension of the IYTSZ, although its interpretation is complicated by the highly oblique convergence of the WMT with SE Asia.

Provenance of the Upper Cretaceous Falam Formation and Paleogene section is inferred to be predominantly from the WPA and Inner Belt, with a secondary continental source that is probably the Naga metamorphic-type basement. There is no indication of, or need for, a source related to Eurasia or India for sediments deposited in the IMR during the Late Cretaceous–Eocene.

Scientific editing by Dhananjai Pandey

Acknowledgements This research formed part of the first author's DPhil dissertation at the University of Oxford, completed in 2021. We thank Day Wa Aung and Tun Naing Zaw, University of Yangon, and Saw Mu Tha Lay Paw (freelance geologist) for their help in planning and organizing the fieldwork. We thank Alexis Licht, Khin Zaw and Jonathan Aitchison for very helpful and constructive reviews that helped to improve this paper.

Author contributions TTN: conceptualization (equal), data curation (lead), formal analysis (lead), funding acquisition (supporting), investigation (lead), methodology (lead), writing – original draft (lead), writing – review & editing (lead); SAR: conceptualization (equal), formal analysis (supporting), funding acquisition (equal), investigation (supporting), methodology (supporting), project administration (equal), supervision (equal), writing – original draft (supporting), writing – review & editing (equal); MPS: conceptualization (equal), formal analysis (supporting), funding acquisition (equal), investigation (supporting), project administration (equal), supervision (equal), writing – original draft (supporting), writing – review & editing (equal); CKM: formal analysis (supporting), investigation (supporting), methodology (supporting), writing – original draft (supporting), writing – review & editing (equal); IM: formal analysis (supporting), funding acquisition (supporting), investigation (supporting), methodology (equal), writing – original draft (supporting), writing – review & editing (equal); ORG: formal analysis (supporting), investigation (supporting), methodology (supporting), supervision (supporting), writing – review & editing (supporting); PRB: formal analysis (supporting), investigation (supporting), methodology (supporting), writing – review & editing (supporting); TD: formal analysis (supporting), investigation (supporting), methodology (supporting), writing – review & editing (supporting); MRP: formal analysis (supporting), investigation (supporting), methodology (supporting), writing – review & editing (supporting); GMH: funding acquisition (equal), methodology (supporting), project administration (equal), supervision (supporting), writing – review & editing (supporting).

Funding This work was primarily funded by Ophir Energy, London, the University of Oxford and the Natural Environment Research Council (NERC) Centre for Doctoral Training in Oil & Gas. The research was supported by a NERC Isotope Geosciences Facility grant-in-kind (IP-1778-1117).

Competing interests The authors declare that they have no known competing financial interests or personal relationships that could have appeared to influence the work reported in this paper.

Data availability All data generated or analysed during this study are included in this published article (and its [Supplementary information files](#)).

References

- Acharyya, S.K. 1986. Tectono-stratigraphic history of Naga Hills Ophiolites. *Geological Survey of India, Memoirs*, **119**, 94–103.
- Acharyya, S.K. 2007. Collisional emplacement history of the Naga–Andaman ophiolites and the position of the eastern Indian suture. *Journal of Asian Earth Sciences*, **29**, 229–242, <https://doi.org/10.1016/j.jseas.2006.03.003>
- Acharyya, S.K. 2015. Indo-Burma Range: a belt of accreted microcontinents, ophiolites and Mesozoic–Paleogene flyschoid sediments. *International Journal of Earth Sciences*, **104**, 1235–1251, <https://doi.org/10.1007/s00531-015-1154-6>
- Advokaat, E.L., Bongers, M.L.M., Rudyawan, A., BouDagher-Fadel, M.K., Langerels, C.G. and van Hinsbergen, D.J.J. 2018. Early Cretaceous origin of the Woyla Arc (Sumatra, Indonesia) by the Australian plate. *Earth and Planetary Science Letters*, **498**, 348–361, <https://doi.org/10.1016/j.epsl.2018.07.001>
- Aitchison, J.C., McDermid, I.R.C., Ali, J.R., Davis, A.M. and Zybrev, S.V. 2007. Shoshonites in southern Tibet record Late Jurassic rifting of a Tethyan intraoceanic island arc. *Journal of Geology*, **115**, 197–213, <https://doi.org/10.1086/510642>
- Aitchison, J.C., Ao, A., Bhowmik, S., Clarke, G.L., Ireland, T.R., Kachovich, S. et al. 2019. Tectonic evolution of the western margin of the Burma microplate based on new fossil and radiometric age constraints. *Tectonics*, **38**, 1718–1741, <https://doi.org/10.1029/2018TC005049>
- Allen, R., Najman, Y. et al. 2008. Provenance of the Tertiary sedimentary rocks of the Indo-Myanmar Ranges, Burma (Myanmar): Burman arc or Himalayan-derived? *Journal of the Geological Society, London*, **165**, 1045–1057, <https://doi.org/10.1144/0016-76492007-143>
- Arboit, F., Min, M., Chew, D., Mitchell, A., Drost, K., Badenszki, E. and Daly, J.S. 2021. Constraining the links between the Himalayan belt and the Central Myanmar basins during the Cenozoic: an integrated multi-proxy detrital geochronology and trace-element geochemistry study. *Geoscience Frontiers*, **12**, 657–676, <https://doi.org/10.1016/j.gsf.2020.05.024>
- Audley-Charles, M.G. 1991. Tectonics of the New Guinea area. *Annual Reviews of Earth and Planetary Sciences*, **19**, 17–41, <https://doi.org/10.1146/annurev.earth.19.050191.000313>
- Bandopadhyay, P., van Hinsbergen, D.J.J. et al. 2022. Paleogeography of the West Burma Block and the eastern Neotethys Ocean: constraints from Cenozoic sediments shed onto the Andaman–Nicobar ophiolites. *Gondwana Research*, **103**, 335–361, <https://doi.org/10.1016/j.gr.2021.10.011>
- Bannert, D., Lyen, A.S. and Than, H. 2011. *The Geology of Indoburman Ranges in Myanmar*. Geologisches Jahrbuch, Reihe B, **101**.
- Barber, A.J. and Crow, M.J. 2005. Pre-Tertiary stratigraphy. *Geological Society, London, Memoirs*, **31**, 24–53, <https://doi.org/10.1144/GSL.MEM.2005.031.01.04>
- Barber, A.J. and Crow, M.J. 2009. Structure of Sumatra and its implications for the tectonic assembly of Southeast Asia and the destruction of Paleotethys. *Island Arc*, **18**, 3–20, <https://doi.org/10.1111/j.1440-1738.2008.00631.x>
- Barber, A.J., Khin, Z. and Crow, M.J. 2017. The pre-Cenozoic tectonic evolution of Myanmar. *Geological Society, London, Memoirs*, **48**, 687–712, <https://doi.org/10.1144/M48.31>
- Baumgartner, P.O., O'Dogherty, L., Gorican, S., Urquhart, E., Pillevert, A. and De Wever, P. 1995. *Middle Jurassic to lower Cretaceous radiolarian of Tethys: occurrences, systematics, biochronology*. Mémoires de Géologie (Lausanne), **23**.
- Baxter, A.T., Aitchison, J.C., Zybrev, S.V. and Ali, J.R. 2011. Upper Jurassic radiolarians from the Naga Ophiolite, Nagaland, northeast India. *Gondwana Research*, **20**, 638–644, <https://doi.org/10.1016/j.gr.2011.02.001>
- Beccaro, P. 2004. Upper Jurassic radiolarians from Inici Mt. area (north-western Sicily, Italy): biochronology and calibration by ammonites. *Rivista Italiana di Paleontologia e Stratigrafia*, **110**, 289–301, <https://doi.org/10.13130/2039-4942/6301>
- Bender, F. 1983. *Geology of Burma*, 1st edn. Gebruder Borntraeger, Berlin-Stuttgart.
- Bertrand, G., Rangin, C. and Maluski, H. 2001. Diachronous cooling along the Mogok metamorphic belt (Shan scarp, Myanmar): the trace of the northward migration of the Indian syntaxis. *Journal of Asian Earth Sciences*, **19**, 649–659, [https://doi.org/10.1016/S1367-9120\(00\)00061-4](https://doi.org/10.1016/S1367-9120(00)00061-4)
- Bhowmik, S.K., Ao, A. and Rajkati, M. 2022. Tectonic framework of the high-pressure metamorphic rocks of the Nagaland Ophiolite Complex, north-east India, and its geodynamic significance: a review. *Geological Journal*, **57**, 727–748, <https://doi.org/10.1002/gj.4248>
- Brunnschweiler, R.O. 1966. On the geology of the Indoburman Ranges. *Journal of the Geological Society of Australia*, **13**, 137–194, <https://doi.org/10.1080/00167616608728608>
- Brunnschweiler, R.O. 1974. Indoburman ranges. *Geological Society, London, Special Publications*, **4**, 279–299, <https://doi.org/10.1144/GSL.SP.2005.004.01.16>
- Cai, F., Ding, L., Laskowski, A.K., Kapp, P., Wang, H., Xu, Q. and Zhang, L. 2016. Late Triassic paleogeographic reconstruction along the Neo–Tethyan Ocean margins, southern Tibet. *Earth and Planetary Science Letters*, **435**, 105–114, <https://doi.org/10.1016/j.epsl.2015.12.027>
- Cai, F., Ding, L., Yao, W., Laskowski, A.K., Xu, Q., Zhang, J. and Kyang, S. 2017. Provenance and tectonic evolution of Lower Paleozoic–Upper Mesozoic strata from Sibumasu terrane, Myanmar. *Gondwana Research*, **41**, 325–336, <https://doi.org/10.1016/j.gr.2015.03.005>
- Cai, F., Ding, L. et al. 2020. Initiation and evolution of forearc basins in the Central Myanmar Depression. *GSA Bulletin*, **132**, 1066–1082, <https://doi.org/10.1130/B35301.1>
- Cao, H., Huang, Y. et al. 2018. Late Triassic sedimentary records in the northern Tethyan Himalaya: tectonic link with Greater India. *Geoscience Frontiers*, **9**, 273–291, <https://doi.org/10.1016/j.gsf.2017.04.001>
- Chhibber, H.L. 1927. The serpentines and associated minerals of the Henzada and Bassein Districts, Burma. *Journal of the Burma Research Society*, **16**, 195–196.
- Chhibber, H.L. 1934. *Geology of Burma*. Macmillan, London.
- Curry, J.R. 2005. Tectonics and history of the Andaman Sea region. *Journal of Asian Earth Sciences*, **25**, 187–228, <https://doi.org/10.1016/j.jseas.2004.09.001>
- Curry, J.R., Moore, D.G., Lawver, L.A., Emmel, F.J., Raitt, R.W., Henry, M. and Kieckhefer, R. 1979. Tectonics of the Andaman Sea and Burma. *AAPG, Memoirs*, **29**, 189–198.
- De Wever, P., Dumitrica, P., Caulet, J.P., Nigrini, C. and Caridroit, M. 2001. *Radiolarians in the Sedimentary Record*. Gordon and Breach, London, <https://doi.org/10.1201/9781482283181>
- Dickinson, W.R. 1985. Interpreting provenance relations from detrital modes of sandstones. *NATO ASI Series*, **148**, 333–361.
- Ding, L., Goswami, T.K., Fulong, C., Barai, U., Sarmah, R.K. and Bezbaruah, D. 2022. Detrital zircon U–Pb ages of Tertiary sequences (Palaeocene–Miocene): Inner Fold Belt and Belt of Schuppen, Indo-Myanmar Ranges, India. *Geological Journal*, **57**, 5191–5206, <https://doi.org/10.1002/gj.4446>
- Fang, D.-R., Wang, G.-H., Hisada, K.-I., Yuan, G.-L., Han, F.-L. and Li, D. 2018. Provenance of the Langjiexue Group to the south of the Yarlung–Tsangpo Suture Zone in southeastern Tibet: insights on the evolution of the Neo-Tethys Ocean in the Late Triassic. *International Geology Review*, **61**, 341–360, <https://doi.org/10.1080/00206814.2018.1425924>
- Fareeduddin, D. and Dilek, Y. 2015. Structure and petrology of the Nagaland–Manipur Hill ophiolitic mélange zone, NE India: a fossil Tethyan subduction channel at the India–Burma plate boundary. *Episodes*, **38**, 298–314, <https://doi.org/10.18814/epiugs/2015/v38i4/82426>
- Gardiner, N.J., Robb, L., Searle, M. and Morley, C.K. 2015. Neotethyan magmatism and metallogeny in Myanmar – an Andean analogue? *Journal of Asian Earth Sciences*, **106**, 197–215, <https://doi.org/10.1016/j.jseas.2015.03.015>
- Gardiner, N.J., Robb, L.J. et al. 2016. The tectonic and metallogenic framework of Myanmar: a Tethyan mineral system. *Ore Geology Reviews*, **79**, 26–45, <https://doi.org/10.1016/j.oregeorev.2016.04.024>
- Gardiner, N.J., Searle, M.P., Robb, L.J., Morley, C.K., Kirkland, C.L. and Spencer, C.J. 2018. The crustal architecture of Myanmar imaged through zircon U–Pb, Lu–Hf and O isotopes: tectonics and metallogenic implications. *Gondwana Research*, **62**, 27–60, <https://doi.org/10.1016/j.gr.2018.02.008>
- Garzanti, E. 2016. From static to dynamic provenance analysis—sedimentary petrology upgraded. *Sedimentary Geology*, **336**, 3–13, <https://doi.org/10.1016/j.sedgeo.2015.07.010>
- Garzanti, E. 2019. Petrographic classification of sand and sandstone. *Earth-Science Reviews*, **190**, 545–563, <https://doi.org/10.1016/j.earscirev.2018.1012.1014>
- Ghose, N.C., Chatterjee, N. and Fareeduddin. 2014. *A Petrographic Atlas of Ophiolite: an Example from the Eastern India–Asia Collision Zone*. Springer.
- Ghosh, B., Pal, T., Bhattacharya, A. and Das, D. 2009. Petrogenetic implications of ophiolite chromite from Rutland Island, Andaman – a boninitic parentage in supra-subduction setting. *Mineralogy and Petrology*, **96**, 59–70, <https://doi.org/10.1007/s00710-008-0039-9>
- Gramann, F. 1974. Some palaeontological data on the Triassic and Cretaceous of the western part of Burma (Arakan Islands, Arakan Yoma, western outcrops of Central Basin). *Newsletters in Stratigraphy*, **3**, 277–290, <https://doi.org/10.1127/nos/3/1974/277>
- Green, O.R., Searle, M.P., Corfield, R.I. and Corfield, R.M. 2008. Cretaceous–Tertiary carbonate platform evolution and the age of the India–Asia collision along the Ladakh Himalaya (northwest India). *Journal of Geology*, **116**, 331–353, <https://doi.org/10.1086/588831>
- Gunawan, I. 2012. Age, character and provenance of the Tipuma Formation, West Papua: new insights from detrital zircon dating. Proceedings Indonesian Petroleum Association 36th Annual Convention, IPA12-G-027, 36th Annual Convention, Jakarta, Indonesia, 1–14.
- Hall, R. 2009. Hydrocarbon basins in SE Asia: understanding why they are there. *Petroleum Geoscience*, **15**, 131–146, <https://doi.org/10.1144/1354-079309-830>
- Hall, R. 2012. Late Jurassic–Cenozoic reconstructions of the Indonesian region and the Indian Ocean. *Tectonophysics*, **570–571**, 1–41, <https://doi.org/10.1016/j.tecto.2012.04.021>
- Hall, R. 2014. The origin of Sundaland. In: Basuki, N.J. and Dahilus, A.Z. (eds) *MGEI Annual Convention. Proceedings of Sundaland Resources, Palembang, South Sumatra, Indonesia*. Masyarakat Geologi Ekonomi Indonesia (Indonesian Society of Economic Geologists), Jakarta, 1–25.
- Harlow, G.E., Tsujimori, T. and Sorensen, S.S. 2015. Jadeitites and plate tectonics. *Annual Review of Earth and Planetary Sciences*, **43**, 105–138, <https://doi.org/10.146/annurev-earth-060614-105215>
- Hébert, R., Bezard, R., Guilmette, C., Dostal, J., Wang, C.S. and Liu, Z.F. 2012. The Indus–Yarlung Zangbo ophiolites from Nanga Parbat to Namche Barwa syntaxes, southern Tibet: first synthesis of petrology, geochemistry, and geochronology with incidences on geodynamic reconstructions of Neo-

- Tethys. *Gondwana Research*, **22**, 377–397, <https://doi.org/10.1016/j.gr.2011.10.013>
- Htay, H., Zaw, K. and Than OoT., 2017. The mafic–ultramafic (ophiolitic) rocks of Myanmar. *Geological Society, London, Memoirs*, **48**, 117–141, <https://doi.org/10.1144/M48.6>
- Huber, B.T., Petrizo, M.R., Young, J.R., Falzoni, F., Gilardoni, S.E., Bown, P.R. and Wade, B.S. 2016. Pforams@microtax. *Micropaleontology*, **62**, 429–438, <https://doi.org/10.47894/mpal.62.6.02>
- Huber, B.T., Petrizo, M.R. and Falzoni, F. 2022. Taxonomy and phylogeny of Albian–Maastrichtian planispiral planktonic foraminifera traditionally assigned to *Globigerinelloides*. *Micropaleontology*, **68**, 117–183, <https://doi.org/10.47894/mpal.68.2.01>
- Hutchinson, C.S. 1989. *Geological Evolution of South East Asia*. Oxford University Press, New York.
- Imchen, W., Thong, G.T. and Pongen, T. 2014. Provenance, tectonic setting and age of the sediments of the Upper Disang Formation in the Phek District, Nagaland. *Journal of Asian Earth Sciences*, **88**, 11–27, <https://doi.org/10.1016/j.jseas.2014.02.027>
- Kapp, P. and DeCelles, P.G. 2019. Mesozoic–Cenozoic geological evolution of the Himalayan–Tibetan orogen and working tectonic hypothesis. *American Journal of Science*, **319**, 159–254, <https://doi.org/10.2475/03.2019.01>
- Khin, K., Sakai, T. and Zaw, K. 2017. Arakan Coastal Ranges in western Myanmar, geology and provenance of Neogene siliciclastic sequences: implication for the tectonic evolution of the Himalaya–Bengal System. *Geological Society, London, Memoirs*, **48**, 81–116, <https://doi.org/10.1144/M48.5>
- Khin, K., Moe, A. and Aung, K.P. 2022. Tectono-structural framework of the Indo-Myanmar Ranges: implications for the structural development on the geology of the Rakhine Coastal Region, Myanmar. *Geosystems and Geoenvironment*, **1**, 100079, <https://doi.org/10.1016/j.geogeo.2022.100079>
- Lamont, T.N., Searle, M.P. *et al.* 2021. Late Eocene–Oligocene granulite facies garnet–sillimanite migmatites from the Mogok metamorphic belt, Myanmar, and implications for timing of slip along the Sagaing Fault. *Lithos*, **386–387**, 106027, <https://doi.org/10.1016/j.lithos.2021.106027>
- Lewis, C.J. and Sircombe, K. 2013. Use of U–Pb geochronology to delineate provenance of North West Shelf Sediments, Australia. Geoscience Australia. In: Keep, M. and Moss, S.J. (eds) *The Sedimentary Basins of Western Australia IV: Proceedings of the Petroleum Exploration Society of Australia Symposium, Perth, WA*. Petroleum Society of Australia, Perth, 1–27.
- Li, J.X., Fan, W.M., Zhang, L.Y., Evans, N.J., Sun, Y.L., Ding, L. and Sein, K. 2019. Geochronology, geochemistry and Sr–Nd–Hf isotopic compositions of Late Cretaceous–Eocene granites in southern Myanmar: petrogenetic, tectonic and metallogenic implications. *Ore Geology Reviews*, **112**, 103031, <https://doi.org/10.1016/j.oregeorev.2019.103031>
- Li, X., Li, Y., Wang, C. and Matsuoka, A. 2013. Late Jurassic radiolarians from the Zhongba Melange in the Yarlung–Tsangpo suture zone, southern Tibet. *Science Reports of Niigata University (Geology)*, **28**, 23–30.
- Licht, A., France-Lanord, C., Reisberg, L., Fontaine, C., Soe, A.N. and Jaeger, J.J. 2013. A palaeo Tibet–Myanmar connection? Reconstructing the Late Eocene drainage system of central Myanmar using a multi-proxy approach. *Journal of the Geological Society, London*, **170**, 929–939, <https://doi.org/10.1144/jgs2012-126>
- Licht, A., Reisberg, L., France-Lanord, C., Naing Soe, A. and Jaeger, J.J. 2016. Cenozoic evolution of the central Myanmar drainage system: insights from sediment provenance in the Minbu Sub-Basin. *Basin Research*, **28**, 237–251, <https://doi.org/10.1111/bre.12108>
- Licht, A., Dupont-Nivet, G. *et al.* 2019. Paleogene evolution of the Burmese forearc basin and implications for the history of India–Asia convergence. *GSA Bulletin*, **131**, 730–748, <https://doi.org/10.1130/B35002.1>
- Licht, A., Win, Z. *et al.* 2020. Magmatic history of central Myanmar and implications for the evolution of the Burma Terrane. *Gondwana Research*, **87**, 303–319, <https://doi.org/10.1016/j.gr.2020.06.016>
- Liu, C.-Z., Zhang, C. *et al.* 2016a. Petrology and geochemistry of mantle peridotites from the Kalemio and Myitkyina ophiolites (Myanmar): implications for tectonic settings. *Lithos*, **264**, 495–508, <https://doi.org/10.1016/j.lithos.2016.09.013>
- Liu, C.-Z., Chung, S.-L. *et al.* 2016b. Tethyan suturing in Southeast Asia: Zircon U–Pb and Hf–O isotopic constraints from Myanmar ophiolites. *Geology*, **44**, 311–314, <https://doi.org/10.1130/G37342.1>
- Lokko, K., Aitchison, J.C., Whiso, K., Lhoupenyi, D., Zhou, R. and Raju, D.S.N. 2020. Eocene foraminifera of the Upper Disang Formation, Naga Hills of Manipur, Indo-Myanmar Range (IMR): implications on age and basin evolution. *Journal of Asian Earth Sciences*, **191**, 104259, <https://doi.org/10.1016/j.jseas.2020.104259>
- Maibam, B., Palin, R.M., Gerdes, A., White, R.W. and Foley, S. 2022. Dating blueschist-facies metamorphism within the Naga ophiolite, northeast India, using sheared carbonate veins. *International Geology Review*, **65**, 378–395, <https://doi.org/10.1080/00206814.2022.2048271>
- Matsuoka, A., Yang, Q., Kobayashi, K., Takei, M., Nagahashi, T., Zeng, Q. and Wang, Y. 2002. Jurassic–Cretaceous radiolarian biostratigraphy and sedimentary environments of the Ceno-Tethys: records from the Xialu Chert in the Yarlung–Zangbo suture zone, southern Tibet. *Journal of Asian Earth Sciences*, **20**, 277–287, [https://doi.org/10.1016/S1367-9120\(01\)00044-X](https://doi.org/10.1016/S1367-9120(01)00044-X)
- Maurin, T. and Rangin, C. 2009. Structure and kinematics of the Indo-Burmese wedge: recent and fast growth of the outer wedge. *Tectonics*, **28**, TC20010, <https://doi.org/10.1029/2008TC002276>
- McDermid, I.R.C., Aitchison, J.C., Davis, A.M., Harrison, M.T. and Grove, M. 2002. The Zedong terrane: a Late Jurassic intra-oceanic magmatic arc within the Yarlung–Tsangpo suture zone, southeastern Tibet. *Chemical Geology*, **187**, 267–277, [https://doi.org/10.1016/S0009-2541\(02\)00040-2](https://doi.org/10.1016/S0009-2541(02)00040-2)
- Metcalf, I. 1990. Allochthonous terrane processes in Southeast Asia. *Philosophical Transactions of the Royal Society of London*, **A331**, 625–640.
- Metcalf, I. 2011. Tectonic framework and Phanerozoic evolution of Sundaland. *Gondwana Research*, **19**, 3–21, <https://doi.org/10.1016/j.gr.2010.02.016>
- Metcalf, I. 2013. Gondwana dispersion and Asian accretion: tectonic and palaeogeographic evolution of eastern Tethys. *Journal of Asian Earth Sciences*, **66**, 1–33, <https://doi.org/10.1016/j.jseas.2012.12.020>
- Mitchell, A.H.G. 1981. Phanerozoic plate boundaries in mainland SE Asia, the Himalayas and Tibet. *Journal of the Geological Society, London*, **138**, 109–122, <https://doi.org/10.1144/gsjgs.138.2.0109>
- Mitchell, A.H.G. 1986. Mesozoic and Cenozoic regional tectonics and metallogenesis in mainland SE Asia. *Geological Society of Malaysia Bulletin*, **20**, 221–239, <https://doi.org/10.7186/bgsm20198612>
- Mitchell, A.H.G. 1989. The Shan Plateau and western Burma: Mesozoic–Cenozoic plate boundaries and correlations with Tibet. *NATO Advanced Science Institute Series*, **259**, 567–583.
- Mitchell, A.H.G. 1992. Late Permian–Mesozoic events and the Mergui Group nappe in Myanmar and Thailand. *Journal of SE Asian Earth Sciences*, **7**, 165–178, [https://doi.org/10.1016/0743-9547\(92\)90051-C](https://doi.org/10.1016/0743-9547(92)90051-C)
- Mitchell, A.H.G. 1993. Cretaceous–Cenozoic tectonic events in the western Myanmar (Burma)–Assam region. *Journal of the Geological Society, London*, **150**, 1089–1102, <https://doi.org/10.1144/gsjgs.150.6.1089>
- Mitchell, A.H.G. 2017. *Geological Belts, Plate Boundaries and Mineral Deposits in Myanmar*. Elsevier, Amsterdam.
- Mitchell, A.H.G., Hlaing, T. and Htay, N. 2010. The Chin Hills segment of the Indo-Myanmar Ranges: not a simple accretionary wedge. *Memoir of the Geological Society of India*, **75**, 3–24.
- Mitchell, A.H.G., Chung, S.L., Oo, T., Lin, T.H. and Hung, C.H. 2012. Zircon U–Pb ages in Myanmar: magmatic–metamorphic events and the closure of a neo-Tethys ocean? *Journal of Asian Earth Sciences*, **56**, 1–23, <https://doi.org/10.1016/j.jseas.2012.04.019>
- Morley, C.K. 2009. Evolution from an oblique subduction back-arc mobile belt to a highly oblique collisional margin: the Cenozoic tectonic development of Thailand and Eastern Myanmar. *Geological Society, London, Special Publications*, **318**, 373–403, <https://doi.org/10.1144/SP318.14>
- Morley, C.K. 2012. Late Cretaceous–early Palaeogene tectonic development of SE Asia. *Earth Science Reviews*, **115**, 37–75, <https://doi.org/10.1016/j.earscirev.2012.08.002>
- Morley, C.K. 2018. Understanding Sibumasu in the context of ribbon continents. *Gondwana Research*, **64**, 184–215, <https://doi.org/10.1016/j.gr.2018.07.006>
- Morley, C.K. and Searle, M.P. 2017. Regional tectonics, structure and evolution of the Andaman–Nicobar Islands from ophiolite formation and obduction to collision and back-arc spreading. *Geological Society, London, Memoirs*, **47**, 51–74, <https://doi.org/10.1144/M47.5>
- Morley, C.K., Naing, T.T., Searle, M.P. and Robinson, S.A. 2020. Structural and tectonic development of the Indo-Burma ranges. *Earth-Science Reviews*, **200**, 102992, <https://doi.org/10.1016/j.earscirev.2019.102992>
- Morley, C.K., Chantpraser, S., Kongchum, J. and Chenoll, K. 2021. The West Myanmar terrane, a review of recent paleo-latitude data, its geological implications and constraints. *Earth-Science Reviews*, **220**, 103722, <https://doi.org/10.1016/j.earscirev.2021.103722>
- Min, M., Ratschbacher, L. *et al.* 2022. India (Tethyan Himalayan Series) in Central Myanmar: implications for the evolution of the Eastern Himalayan Syntaxis and the Sagaing transform-fault system. *Geophysical Research Letters*, **49**, e2022GL099140, <https://doi.org/10.1029/2022GL099140>
- Naing, T.T., Bussien, D.A., Winkler, W., Nold, M. and von Quadt, A. 2014. Provenance study on Eocene–Miocene sandstones of the Rakhine Coastal Belt, Indo-Myanmar Ranges of Myanmar: geodynamic implications. *Geological Society, London, Special Publications*, **386**, 195–216, <https://doi.org/10.1144/SP386.10>
- Najman, Y., Sobel, E.R. *et al.* 2020. The exhumation of the Indo-Myanmar Ranges, Myanmar. *Earth and Planetary Science Letters*, **530**, 115948, <https://doi.org/10.1016/j.epsl.2019.115948>
- Najman, Y., Sobel, E.R. *et al.* 2022. The timing of collision between Asia and the West Myanmar terrane, and the development of the Indo-Burman Ranges. *Tectonics*, **41**, e2021TC007057, <https://doi.org/10.1029/2021TC007057>
- Ningthoujam, P.S., Dubey, C.S., Guillot, S., Fagion, A.-S. and Shukla, D.P. 2012. Origin and serpentinization of ultramafic rocks of Manipur Ophiolite Complex in the Indo-Myanmar subduction zone, Northeast India. *Journal of Asian Earth Sciences*, **50**, 128–140, <https://doi.org/10.1016/j.jseas.2012.01.004>
- Niu, X., Liu, F., Yang, J., Dilek, Y., Xu, Z. and Sein, K. 2018. Mineralogy, geochemistry, and melt evolution of the Kalemio peridotite massif in the Indo-Myanmar Ranges (western Myanmar), and tectonic implications. *Lithosphere*, **10**, 79–94, <https://doi.org/10.1130/L589.1>
- Pal, T. 2011. Petrology and geochemistry of the Andaman ophiolite: melt-rock interaction in a suprasubduction-zone setting. *Journal of the Geological Society, London*, **168**, 1031–1045, <https://doi.org/10.1144/0016-76492009-152>

- Pedersen, R.-B., Searle, M.P., Carter, A. and Bandopadhyay, P.C. 2010. U–Pb zircon age of the Andaman ophiolite: implications for the beginning of subduction beneath the Andaman–Sumatra arc. *Journal of the Geological Society, London*, **167**, 1105–1112, <https://doi.org/10.1144/0016-76492009-151>
- Pessagno, E.A. and Newport, R.L. 1972. A technique for extracting Radiolaria from radiolarian cherts. *Micropaleontology*, **18**, 231–234, <https://doi.org/10.2307/1484997>
- Pivnik, D.A., Nahm, J., Tucker, R.S., Smith, G.O., Nyein, K., Nyunt, M. and Maung, P.H. 1998. Polyphase deformation in a fore-arc/back-arc basin, Salin Subbasin, Myanmar (Burma). *AAPG Bulletin*, **82**, 1837–1856.
- Poinar, G. 2019. Burmese amber: evidence of Gondwanan origin and Cretaceous dispersion. *Historical Biology*, **31**, 1304–1309, <https://doi.org/10.1080/08912963.2018.1446531>
- Rangin, C. 2017. Active and recent tectonics of the Burma Platelet in Myanmar. *Geological Society, London, Memoirs*, **48**, 53–64, <https://doi.org/10.1144/M48.3>
- Rangin, C. 2018. *The Western Sunda Basins, and the India/Asia Collision: an Atlas*. Geotecton Consulting.
- Rangin, C., Maurin, T. and Masson, F. 2013. Combined effects of Eurasia/Sunda oblique convergence and East-Tibetan crustal flow on the active tectonics of Burma. *Journal of Asian Earth Sciences*, **76**, 185–194, <https://doi.org/10.1016/j.jseas.2013.05.018>
- Sarkar, A., Datta, A.K., Poddar, B.C., Bhattacharyya, B.K., Kollapuri, V.K. and Sanwal, R. 1996. Geochronological studies of Mesozoic igneous rocks from eastern India. *Journal of Southeast Asian Earth Sciences*, **13**, 77–81, [https://doi.org/10.1016/0743-9547\(96\)00009-8](https://doi.org/10.1016/0743-9547(96)00009-8)
- Searle, M.P. and Morley, C.K. 2011. Tectonic and thermal evolution of Thailand in the regional context of SE Asia. In: Ridd, M.F., Barber, A.J. and Crow, M.J. (eds) *The Geology of Thailand*. Geological Society, London, 539–571, <https://doi.org/10.1144/GOTH.20>
- Searle, M.P., Noble, S.R., Cottle, J.M., Waters, D.J., Mitchell, A.H.G., Hlaing, T. and Horstwood, M.S.A. 2007. Tectonic evolution of the Mogok metamorphic belt, Burma (Myanmar) constrained by U–Th–Pb dating of metamorphic and magmatic rocks. *Tectonics*, **26**, TC3014, <https://doi.org/10.1029/2006TC002083>
- Searle, M.P., Morley, C.K., Waters, D.J., Gardiner, N.J., Htun, U.K., Nu, T.T. and Robb, L.J. 2017. Tectonic and metamorphic evolution of the Mogok Metamorphic and Jade Belts, and ophiolitic terranes of Burma (Myanmar). *Geological Society, London, Memoirs*, **48**, 263–295, <https://doi.org/10.1144/M48.12>
- Searle, M.P., Garber, J.M., Hacker, B.R., Htun, K., Gardiner, N.J., Waters, D.J. and Robb, L.J. 2020. Timing of syenite–charnockite magmatism and ruby and sapphire metamorphism in the Mogok valley region, Myanmar. *Tectonics*, **39**, e2019TC005998, <https://doi.org/10.1029/2019TC005998>
- Sengör, A.M.C. 1987. Tectonics of the Tethysides: orogenic collage development in a collisional setting. *Annual Reviews of Earth and Planetary Sciences*, **15**, 213–244, <https://doi.org/10.1146/annurev.earth.15.050187.001241>
- Sevastjanova, I., Hall, R., Rittner, M., Paw, S.M.T.L., Naing, T.T., Alderton, D.H. and Comfort, G. 2016. Myanmar and Asia united, Australia left behind long ago. *Gondwana Research*, **32**, 24–40, <https://doi.org/10.1016/j.gr.2015.02.001>
- Singh, A.K. 2013. Petrology and geochemistry of Abyssal Peridotites from the Manipur Ophiolite Complex, Indo-Myanmar Orogenic Belt, northeast India. Implication for melt generation in mid-oceanic ridge environment. *Journal of Asian Earth Sciences*, **66**, 258–276, <https://doi.org/10.1016/j.jseas.2013.02.004>
- Singh, A.K., Chung, S.-L., Bikramaditya, R.K. and Lee, H.Y. 2017. New U–Pb zircon ages of plagiogranites from the Nagaland-Manipur ophiolites, Indo-Myanmar Orogenic Belt, NE India. *Journal of the Geological Society*, **174**, 170–179, <https://doi.org/10.1144/jgs2016-048>
- Sloan, R.A., Elliott, J.R., Searle, M.P. and Morley, C.K. 2017. Active tectonics of Myanmar and the Andaman Sea. *Geological Society, London, Memoirs*, **48**, 19–52, <https://doi.org/10.1144/M48.2>
- Socquet, A., Goffé, B., Pubellier, M. and Rangin, C. 2002. Le métamorphisme Tardi-Crétacé à Eocène des zones internes de la chaîne Indo-Birmanne (Burma occidentale): implication géodynamique. *Comptes Rendus, Geosciences*, **334**, 573–580, [https://doi.org/10.1016/S1631-0713\(02\)01796-0](https://doi.org/10.1016/S1631-0713(02)01796-0)
- Soe, T.T., Maung, T., Nyunt, H. and Kyaing, S. 2014. *Geological Map of Myanmar, 2014. Scale 1:2,250,000*. Myanmar Geosciences Society.
- Steckler, M.S., Akhter, S.H. and Seeber, L. 2008. Collision of the Ganges–Brahmaputra Delta with the Burma Arc: implications for earthquake hazard. *Earth and Planetary Science Letters*, **273**, 367–378, <https://doi.org/10.1016/j.epsl.2008.07.009>
- Steckler, M.S., Mondal, D.R. et al. 2016. Locked and loading metathrust linked to active subduction beneath the Indo-Myanmar Ranges. *Nature Geoscience*, **9**, 615–618, <https://doi.org/10.1038/ngeo2760>
- Suzuki, H., Maung, M., Aung, A.K. and Takai, M. 2004. Jurassic radiolaria from chert pebbles of the Eocene Pondaung Formation, Central Myanmar. *Neues Jahrbuch für Geologie und Paläontologie-Abhandlungen*, **231**, 369–393, <https://doi.org/10.1127/njgpa/231/2004/369>
- Theobald, W. 1871. The axial group in Western Prome, British Burmah. *Geological Survey of India Records (Calcutta)*, **4**, 33–44.
- Tun, S.T. and Watkinson, I.M. 2017. The Sagaing Fault, Myanmar. *Geological Society, London, Memoirs*, **48**, 415–443, <https://doi.org/10.1144/M48.19>
- United Nations 1979. *Geology and Exploration Geochemistry of part of the Northern and Southern Chin Hills and Arakan Yoma, Western Burma*. Technical Report 4. United Nations Development Programme **DP/UN/BUR-72-002/13**. United Nations, New York.
- Veevers, J.J. 1988. Morphotectonics of Australia's northwestern margin – a review. In: Purcell, P.G. and Purcell, R.R. (eds) *The North West Shelf Proceedings of Petroleum Exploration Society of Australia Symposium*. PESA, Perth, WA, 19–27.
- Wang, J.G., Wu, F.Y., Tan, X.-C. and Liu, C.-Z. 2014. Magmatic evolution of the Western Myanmar Arc documented by U–Pb and Hf isotopes in detrital zircon. *Tectonophysics*, **612**–**613**, 97–105, <https://doi.org/10.1016/j.tecto.2013.11.039>
- Wang, J.G., Wu, F.Y., Garzanti, E., Hu, X., Ji, W.Q., Liu, Z.C. and Liu, X.C. 2016. Upper Triassic turbidites of the northern Tethyan Himalaya (Langjixue Group): the terminal of a sediment-routing system sourced in the Gondwanide Orogen. *Gondwana Research*, **34**, 84–98, <https://doi.org/10.1016/j.gr.2016.03.005>
- Westerweel, J. 2020. *The India–Asia Collision from the Perspective of Myanmar: Insights from Paleomagnetism and Paleogeographic Reconstructions*. PhD thesis, University of Rennes.
- Westerweel, J., Roperch, P., Licht, A., Dupont-Nivet, G., Win, Z., Poblete, F. and Aung, D.W. 2019. Burma Terrane part of the Trans-Tethyan arc during collision with India according to palaeomagnetic data. *Nature Geoscience*, **12**, 863–868, <https://doi.org/10.1038/s41561-019-0443-2>
- Westerweel, J., Licht, A. et al. 2020. Burma terrane collision and northward indentation in the Eastern Himalayas recorded in the Eocene–Miocene Chindwin Basin (Myanmar). *Tectonics*, **39**, e2020TC006413, <https://doi.org/10.1029/2020TC006413>
- Yang, J.-S., Xu, Z.Q. et al. 2012. Discovery of a Jurassic SSZ ophiolite in the Myitkyina region of Myanmar. *Acta Petrological Sinica*, **28**, 1710–1730.
- Yang, S., Liang, X. et al. 2022. Slab remnants beneath the Myanmar terrane evidencing double subduction of the Neo-Tethyan Ocean. *Scientific Advances*, **8**, eabo1027, <https://doi.org/10.1126/sciadv.abo1027>
- Yao, W., Ding, L., Cai, F., Wang, H., Xu, Q. and Zaw, T. 2017. Origin and tectonic evolution of upper Triassic turbidites in the Indo-Myanmar Ranges, West Myanmar. *Tectonophysics*, **721**, 90–105, <https://doi.org/10.1016/j.tecto.2017.09.016>
- Zhang, J., Xiao, W. et al. 2018. Multiple alternating forearc- and backarc-ward migration of magmatism in the Indo-Myanmar orogenic belt since the Jurassic: documentation of the orogenic architecture of eastern Neotethys in SE Asia. *Earth Science Reviews*, **185**, 704–731, <https://doi.org/10.1016/j.earscirev.2018.07.009>
- Zhang, J.E., Xiao, W., Windley, B.F., Cai, F., Sein, K. and Naing, S. 2017. Early Cretaceous wedge extrusion in the Indo-Burma Range accretionary complex: implications for the Mesozoic subduction of Neotethys in SE Asia. *International Journal of Earth Science*, **106**, 1391–1408, <https://doi.org/10.1007/s0053101714687>
- Zhang, P., Mei, L., Hu, X., Li, R., Wu, L., Zhou, Z. and Qiu, H. 2017. Structure, uplift, and magmatism of the Western Myanmar Arc: constraints to mid-Cretaceous–Paleogene tectonic evolution of the western Myanmar continental margin. *Gondwana Research*, **52**, 18–38, <https://doi.org/10.1016/j.gr.2017.09.002>
- Zhang, P., Najman, Y. et al. 2019. Palaeodrainage evolution of the large rivers of East Asia, and Himalayan–Tibet tectonics. *Earth-Science Reviews*, **192**, 601–630, <https://doi.org/10.1016/j.earscirev.2019.02.003>
- Zhang, X., Chung, S.-L. et al. 2021. Tracing Argoland in eastern Tethys and implications for India–Asia convergence. *GSA Bulletin*, **133**, 1712–1722, <https://doi.org/10.1130/B35772.1>